Powdery mildew effectors AVR_{A1} and BEC1016 target the ER J-domain protein *Hv*ERdj3B required for immunity in barley

Running title: Two powdery mildew effectors target barley ERdj3B

Zizhang Li[1], Valeria Velásquez-Zapata[2,3], J. Mitch Elmore[3,4,#], Xuan Li[1], Wenjun Xie[1], Sagnik Banerjee[2,4], Hans J. L. Jørgensen[1], Carsten Pedersen[1], Roger P. Wise[2,3,5], Hans Thordal-Christensen[1]

[1)]Department of Plant and Environmental Sciences, University of Copenhagen, Thorvaldsensvej 40, 1871 Frederiksberg C, Denmark

[2)]Program in Bioinformatics & Computational Biology, Iowa State University, Ames, Iowa, 50011, USA

[3)]Department of Plant Pathology & Microbiology, Iowa State University, Ames, Iowa, 50011 USA

[4)] Department of Statistics, Iowa State University, Ames, Iowa, 50011, USA

[5)]Corn Insects and Crop Genetics Research Unit, USDA-Agricultural Research Service, Ames, Iowa, 50011, USA

Authors for correspondence: roger.wise@usda.gov and htc@plen.ku.dk

[#]Present Address: USDA-Agricultural Research Service, Cereal Disease Laboratory, 1551 Lindig Street, St. Paul, MN 55108, USA

ORCID IDs
Zizhang Li: 0000-0001-7818-5162
Valeria Velásquez-Zapata: 0000-0002-2756-2156
J. Mitch Elmore: 0000-0003-4068-0373
Xuan Li: 0000-0001-9338-0150
Wenjun Xie: 0000-0001-8101-5519
Sagnik Banerjee: 0000-0002-2052-7577
Hans J. L. Jørgensen: 0000-0002-5902-6550
Carsten Pedersen: 0000-0002-9520-2232
Roger P. Wise: 0000-0001-7786-1528
Hans Thordal-Christensen: 0000-0001-8813-0157

ABSTRACT

Plant disease resistance often occurs upon direct or indirect recognition of pathogen effectors by host nucleotide-binding leucine-rich-repeat (NLR) receptors. The barley powdery mildew fungus, *Blumeria graminis* f. sp. *hordei* (*Bgh*), secretes hundreds of candidate secreted effector proteins (CSEPs) to facilitate pathogen infection and colonization. One of these, CSEP0008, is directly recognized by the barley NLR, MLA1, and therefore designated AVR_{A1}. Here we show that AVR_{A1} and the sequence-unrelated *Bgh* effector BEC1016 (CSEP0491) suppress immunity in barley cells. We then used yeast 2-hybrid next-generation-interaction screens (Y2H-NGIS), followed by binary Y2H and bimolecular fluorescence complementation, to identify a common barley target of AVR_{A1} and BEC1016, the endoplasmic reticulum (ER)-localized J-domain protein, *Hv*ERdj3B. This is an ER protein quality control (ERQC) protein and silencing it increased the *Bgh* penetration rate in barley. *Hv*ERdj3B is localized to the ER lumen, and AVR_{A1} and BEC106 translocation into the ER was confirmed using a split GFP system. Together, these results suggest that the barley innate immunity, preventing *Bgh* entry into epidermal cells, is dependent on ERQC, which in turn is regulated by J-domain protein *Hv*ERdj3B and the two effectors. Previous work has shown that AVR_{A1} is directly recognized in the cytosol by the immune receptor, MLA1. We speculate whether the AVR_{A1} J-domain target being inside the ER, where it is inapproachable by NLRs, has forced the plant to evolve this challenging direct recognition.

INTRODUCTION

Plants have evolved a multilayered and interconnected innate immune system to protect themselves against pathogen attacks (Yuan et al., 2021a, Ngou et al., 2022). An initial layer, designated pathogen-associated molecular pattern-triggered immunity (PTI) is activated by pattern-recognition receptors (PRRs) located on the plasma membrane (PM) (Zipfel and Oldroyd, 2017). However, plant pathogens can secrete large numbers of effectors into the host to interfere with many host cellular processes in order to suppress PTI and establish parasitism (Kanja and Hammond-Kosack, 2020; Figueroa et al., 2021). In response, plants have evolved an additional interconnected system, termed effector-triggered immunity (ETI) that is initiated upon direct or indirect recognition of effectors by specific intracellular nucleotide-binding leucine-rich repeat

65 (NLR) receptors (Jones *et al*., 2016; Thordal-Christensen, 2020; Ngou *et al*., 2022). With some
66 exceptions, NLR receptors represent the most utilized class of resistance proteins in agriculture
67 (Sun *et al.*, 2020; van Wersch et al., 2020; Kourelis and van der Hoorn, 2018; Ngou et al., 2022).
68 These innate immune systems rely on basic cellular processes, such as protein quality control
69 systems. An intact endoplasmic reticulum (ER) quality control (ERQC) is required to transport
70 certain *de novo* synthesized PRRs through the ER for them to be trafficked to their destination at
71 the PM (Tintor and Saijo, 2014). For example, trafficking of the Arabidopsis EF-Tu receptor, EFR, is
72 particularly dependent on the ERQC, where it requires the chaperones, ER DnaJ3B protein
73 (ERdj3B) and binding immunoglobulin protein 3 (BiP3), as well as stromal cell-derived factor 2
74 (SDF2), for its proper folding and glycosylation (Nekrasov et al., 2009). ERdj3B is an ER luminal J-
75 domain protein, but J-domain proteins elsewhere in the cell have been implicated in plant
76 immunity as well. For instance, in rice infected by the blast fungus, *Magnaporthe oryzae*, cytosolic
77 and mitochondria-associated J-domain proteins are essential for immunity, and interestingly, the
78 latter protein is targeted by a disease-promoting, fungal effector (Zhong et al., 2018; Xu et al.,
79 2020a). J-domain proteins are related to the bacterial DnaJ chaperones, also known as heat shock
80 proteins 40 (HSP40). They interact with HSP70 proteins, such as BiP in the ER, to which they
81 deliver misfolded client proteins and stimulate the HSP70 ATPase activity (Pobre et al., 2019;
82 Fatima et al., 2021).
83 Several recent genomics, transcriptomics and proteomics studies have identified up
84 to 600 candidates for secreted effector proteins (CSEPs) in the barley powdery mildew fungus,
85 *Blumeria graminis* f. sp. *hordei* (*Bgh*) (Bindschedler et al., 2009; Spanu et al., 2010; Pedersen et al.,
86 2012; Menardo et al., 2017; Frantzeskakis et al., 2018). However, only a subset of these have been
87 studied in detail. Host-induced gene silencing (HIGS) analyses have demonstrated that
88 approximately 20 CSEPs contribute to *Bgh* virulence, which is ~25% of those studied (Zhang et al.,
89 2012; Pliego et al., 2013; Ahmed et al., 2015; 2016; Aguilar et al., 2016; Li et al., 2021; Yuan et al.,
90 2021b). Li et al. (2021) screened ~100 CSEPs from *Bgh* and found 15 of them to suppress BAX-
91 induced programmed cell death in *Nicotiana benthamiana*. Two of those, CSEP0139 and
92 CSEP0182, also suppressed BAX-induced programmed cell death in barley. To date, only a few
93 plant targets of *Bgh* effectors have been identified. CSEP0055 targets the barley defense proteins,
94 PR1 and PR17 (Zhang et al., 2012), while CSEP0105 and CSEP0162 target the barley small heat

95 shock proteins, Hsp16.9 and Hsp17.5 (Ahmed et al., 2015). CSEP0064 and CSEP0264 target PR10,
96 while CSEP0264, historically designated Blumeria effector candidate (BEC)1054, also targets
97 eukaryotic elongation factor1 alpha (Pennington et al., 2019). In addition, CSEP0027 was recently
98 found to target a barley catalase (Yuan et al., 2021b).

99 In addition to virulence functions, six *Bgh* CSEPs are directly recognized as avirulence
100 proteins by NLRs encoded by an allelic series of the *Mla* powdery mildew resistance locus
101 (Seeholzer *et al*. 2010; Lu et al., 2016; Saur et al., 2019; Bauer et al., 2021). For instance, CSEP0008
102 (gene ID BLGH_03023) is recognized by MLA1, and thus named AVR_{A1} (Lu et al., 2016). Other
103 recognized CSEPs are CSEP0059 (AVR_{A7}), CSEP0174 (AVR_{A9}), CSEP0141 (AVR_{A10} and AVR_{A22}), and
104 CSEP0372 (AVR_{A13}) (Lu et al., 2016; Saur et al., 2019; Bauer et al., 2021).

105 In this investigation, we were interested in discerning host targets for AVR_{A1}
106 (CSEP0008, gene ID BLGH_03023) (Lu et al., 2016) and BEC1016 (CSEP0491, gene ID BLGH_07006)
107 (Pliego et al. 2013), as examples of effectors with avirulence and virulence functions in barley-*Bgh*
108 interactions, respectively. Recent advances in yeast 2-hybrid (Y2H) analyses, termed next-
109 generation-interaction screening (NGIS) (Suter et al. 2015), use deep sequencing to score the
110 output from Y2H screens (Erffelinck et al., 2018; Lewis et al., 2012, Pashkova et al., 2016; Trigg et
111 al., 2017; Weimann et al., 2013; Yachie et al., 2016). These approaches facilitate a quantitative
112 measure of which preys interact with each bait protein (Suter et al. 2015) and identify
113 reproducible protein-protein interactions (PPI**)** with 70-90% accuracy (Pashkova et al., 2016; Trigg
114 et al., 2017; Weimann et al., 2013; Velásquez-Zapata et al., 2021). This then allows functional PPI
115 to be positioned within interactome networks (Mukhtar et al., 2011; Weßling et al., 2014;
116 Velásquez-Zapata et al., 2021; 2022).

117 We used AVR_{A1} and BEC1016 as baits to conduct NGIS with a Y2H prey library
118 developed from a barley-*Bgh* infection time course and identified the barley J-containing protein,
119 *Hv*ERdj3B, as a host target for both effectors. Our analyses revealed that *Hv*ERdj3B is an ER-
120 luminal protein and using a split GFP system we could show that both effectors translocate signal
121 peptide (SP)-independently from the plant cytosol into the ER lumen. Silencing *Hv*ERdj3B, as well
122 as overexpression of AVR_{A1} and BEC1016, enhanced the formation of fungal haustoria. Together,
123 our results indicate an essential role of ERQC in barley innate immunity and suggest that *Bgh*
124 effectors can interfere with ERQC processes.

125

126

127

128 **RESULTS**

129 **AVR_{A1} and BEC1016 effectors contribute to *Bgh* infection**

130 The two effector candidates AVR_{A1} (singleton) and BEC1016 (CSEP family 5) (Pedersen et al., 2012)
131 are non-homologous in protein sequence, but both belong to the superfamily of RNase-like
132 proteins associated with haustoria (RALPH) effectors with features resembling catalytically inactive
133 RNases (Spanu, 2017) (**Supplemental Figure S1**). They were selected as examples of *Bgh* proteins
134 with documented avirulence and virulence functions, respectively. As an avirulence protein
135 recognized by MLA1, AVR_{A1} is predicted also to have virulence function. However, this could not
136 be documented using HIGS, unlike the case for BEC1016 (Pliego et al., 2013). Both effectors display
137 increased transcript abundance in compatible interactions on *mla6*-18982 mutant plants
138 (Chapman et al., 2021) as compared to incompatible interactions on its resistant CI 16151 (*Mla6*)
139 progenitor (**Supplemental Figure S2**), which supports their role in virulence. As an alternative
140 approach to study virulence functions, we transiently over-expressed AVR_{A1} and BEC1016 (w/o SP)
141 in leaf epidermal cells of one-week-old Golden Promise (susceptible) barley plants using particle
142 bombardment. Two days later, the leaves were inoculated with *Bgh*, and after another 2 days
143 transformed cells were scored for presence of a fungal feeding structure, termed haustorium, as
144 evidence for successful penetration and fungal infection. Our data revealed that AVR_{A1} and
145 BEC1016 significantly increased *Bgh* penetration, resulting in 96% and 150% higher haustoria
146 numbers, respectively (**Figure 1A**).

147 Pathogen-induced callose depositions function as a chemical and physical reinforcement of the
148 plant cell wall towards invading pathogens (Voigt, 2014). To determine whether AVR_{A1} and
149 BEC1016 affect callose deposition, they were introduced into barley leaf cells using EtHAn, a strain
150 of *Pseudomonas fluorescens* modified to express the type-3 secretion system (T3SS) (Thomas et
151 al., 2009; Upadhyaya et al., 2014). To verify protein transfer to the barley cells, EtHAn transformed
152 with a construct expressing β-glucoronidase (GUS) fused to a signal peptide for T3SS resulted in
153 clear blue staining of the leaf cells after reaction buffer incubation (**Supplemental Figure S3**).
154 While EtHAn itself triggers callose formation, it can at the same time be studied how this is
155 influenced by effectors (Sohn et al., 2007; Xu et al., 2020b). Five replicates of eight-day-old Golden
156 Promise first leaves were infiltrated with EtHAn expressing GUS (negative control), AVR_{A1} or

Powdery mildew effectors AVR_{A1} and BEC1016 target the ER J-domain protein *Hv*ERdj3B required for immunity in barley

Figure 1

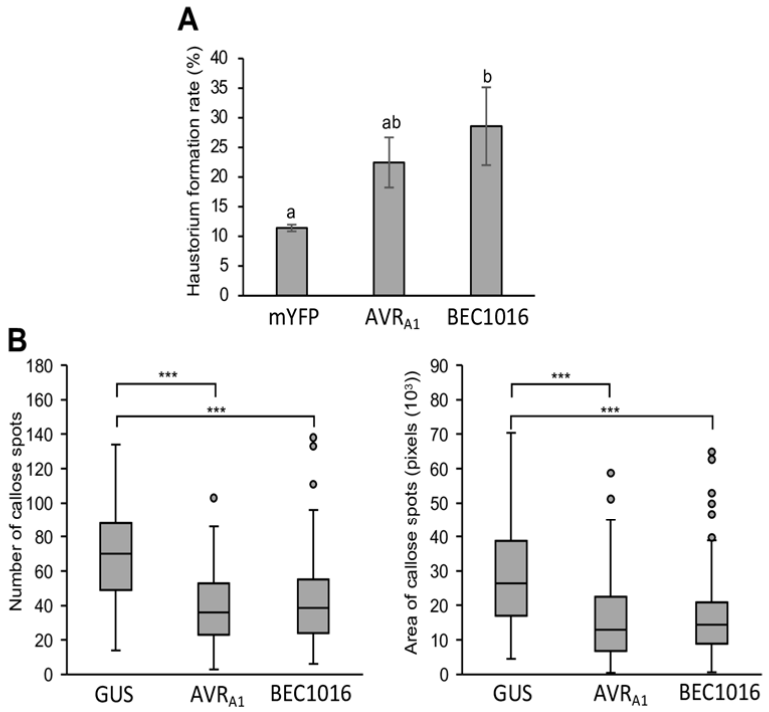

Figure 1. Influence of AVR_{A1} and BEC1016 on *Bgh* infection and callose deposition in barley. A, Effect of transient over-expression of AVR_{A1} and BEC1016 on *Bgh* invasion. pUbi promoter-driven over-expression constructs were co-bombarded with a GUS-reporter constructs into leaf epidermal cells of 1-week-old barley and 2 days later inoculated with *Bgh*. After another 2 days, the fungal haustorium formation was scored in GUS expressing cells. Data shown are mean values of three independent experiments. Error bars, SE. Letters (a, ab and b) indicate significant differences calculated using a logistic regression model (P = 0.0179). **B,** AVR_{A1} and BEC1016 can reduce bacterium-triggered callose deposition in barley plants estimated as numbers of callose spots (left) and area of callose spots (right). Leaves of eight-day-old barley plants were infiltrated with EtHAn, transformed with pEDV6-GUS, pEDV6-AVR_{A1} or pEDV6-BEC1016, and 24 h later the callose deposition we scored. Boxplots for the total number and total area of callose depositions show data for all pictures taken across biological replicates under each treatment. A repeated measures ANOVA followed for a paired sample t test were used to compare the treatments. ***, $P < 2x10^{-16}$. Data shown are based on five independent experiments, statistically treated as replicates.

157 BEC1016. After 24 h, both the total number and total area of callose depositions were significantly

158 reduced by the effectors (**Figure 1B**). Taken together, it appears that AVR_{A1} and BEC1016 target
159 and inhibit PTI, and thereby promote *Bgh* penetration.

160 **Both AVR_{A1} and BEC1016 interact with barley J-domain protein, *Hv*ERdj3B**

161 To identify barley targets for AVR_{A1} and BEC1016, batch Y2H-NGIS was performed according to
162 Velásquez-Zapata et al. (2021). The screens involved parallel histidine selection vs. non-selection
163 and bait specificity to enrich for yeast cells expressing interacting bait and prey proteins.
164 Sequencing reads across the GAL4 activation domain (AD) coding sequence into the prey protein
165 coding sequences were performed on all cultures. We recently developed two complementary
166 software packages, designated NGPINT and Y2H-SCORES, to quantify the outcome of Y2H-NGIS
167 (Banerjee et al., 2021; Velásquez-Zapata et al., 2021). NGPINT facilitates the identification of GAL4
168 AD-prey *in-frame* coding sequence fusion reads. Then Y2H-SCORES uses count data to build a set
169 of ranking scores to predict three properties expected from true interactors, *i.e.*, enrichment in
170 selection vs. non-selection conditions, specificity to a bait screening, and *in-frame* selection of the
171 prey (Velásquez-Zapata et al., 2021). Prey proteins that interact with the selected baits, as
172 indicated by significant enrichment under selection, are reconstituted *in silico* with their mapped
173 fusion reads to identify the complete prey sequence containing the PPI domain for further studies.

174 Using AVR_{A1} and BEC1016 effectors as baits to screen a 3-frame Y2H library made
175 from our infection time course (Banerjee et al 2021; Velásquez-Zapata et al., 2021) we identified
176 HORVU.MOREX.r2.1HG0019270, herein designated *Hv*ERdj3B, as a candidate interactor for both
177 (**Figure 2**). A ranking (**Supplemental Table S1**) and visualization of the interactor candidates of
178 each bait allowed the identification of a prey fragment covering the C-terminal two-thirds of
179 *Hv*ERdj3B (aa 142-350). Binary Y2H according to Dreze *et al*. (2010) confirmed its interaction with
180 AVR_{A1} and BEC1016 (**Supplemental Figure S4**).

181 To study the specificity of these interactions further, extensive binary Y2H assays
182 were performed. The two effectors (w/o SP) were fused to either the Gal4 transcription factor
183 DNA-binding domain (BD) or transcription-activation domain (AD) and combined with either the
184 full-length (w/o SP), the C-terminal two-thirds (aa 142-350) or the central part (aa 142-231) of
185 *Hv*ERdj3B fused to either the AD or the BD. In both orientations of the setup, both effectors were
186 found to interact with the C-terminal two-thirds and the central part, but not the full-length of

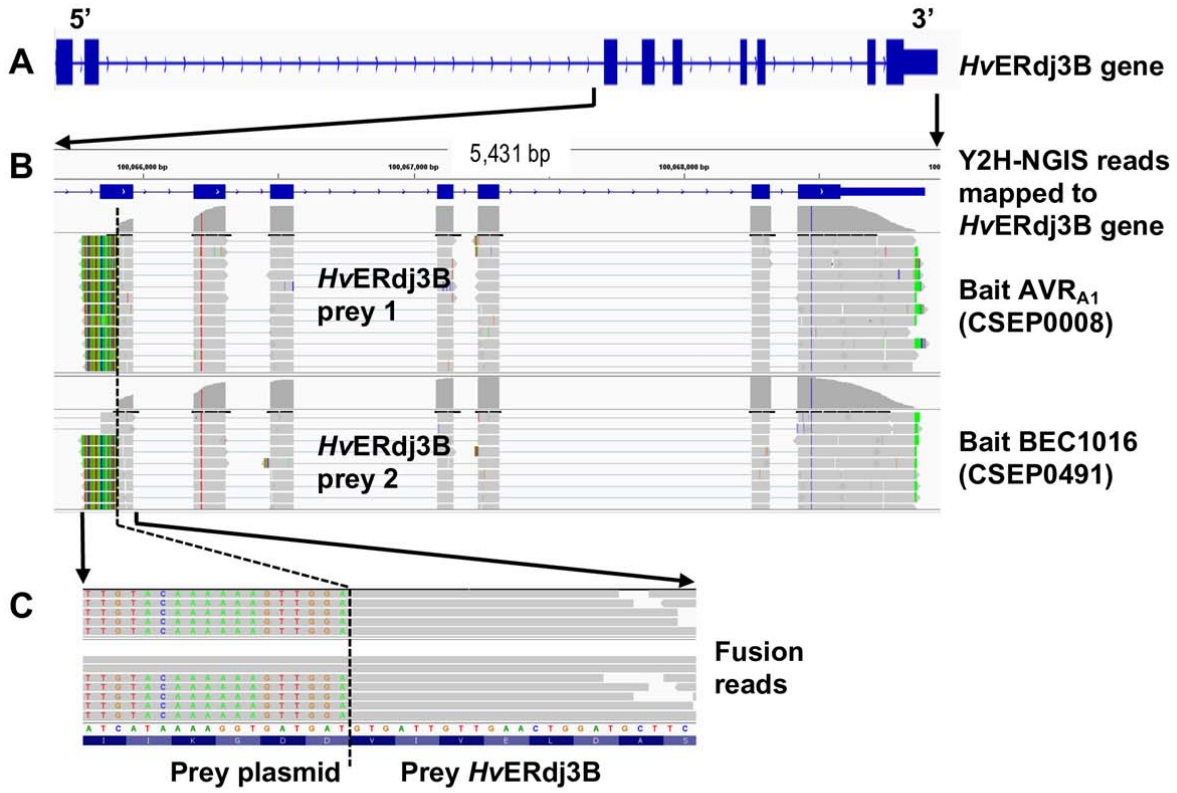

Figure 2. Y2H-NGIS used to identify interactions between AVR_{A1}, BEC1016 and *Hv*ERdj3B. A, *Hv*ERdj3B gene model with exons depicted as blue boxes and introns as hash marks. **B,** Integrative genomic view (IGV) obtained from the software NGPINT after Y2H-NGIS analysis of the *Hv*ERdj3B prey reads selected by both the AVR_{A1} and the BEC1016 bait. Prey fragments were reconstructed from the reads mapped to the *HvERdj3B* gene (shown in grey across the exons) in each Y2H-NGIS dataset and located towards the 3' end of the gene in both cases. **C,** Expanded view of the 5' fusion reads that allowed the determination of the frame and nucleotide-resolved prey fragments. The fusion reads contain a prey plasmid sequence (shown in different colors as mismatches from the reference gene) and the prey sequence.

*Hv*ERdj3B (**Figure 3)**. This suggests that the binding occurs only at the central part of *Hv*ERdj3B, and explains why reads did not appear from the 5' end of the coding sequence in the Y2H-NGIS sequencing results.

To confirm these interactions *in planta*, a bimolecular fluorescence complementation (BiFC) assay (Hu et al., 2002) was carried out in *N. benthamiana* leaf epidermal cells after Agrobacterium-mediated transformation. In this study, only the full-length *Hv*ERdj3B (w/o signal

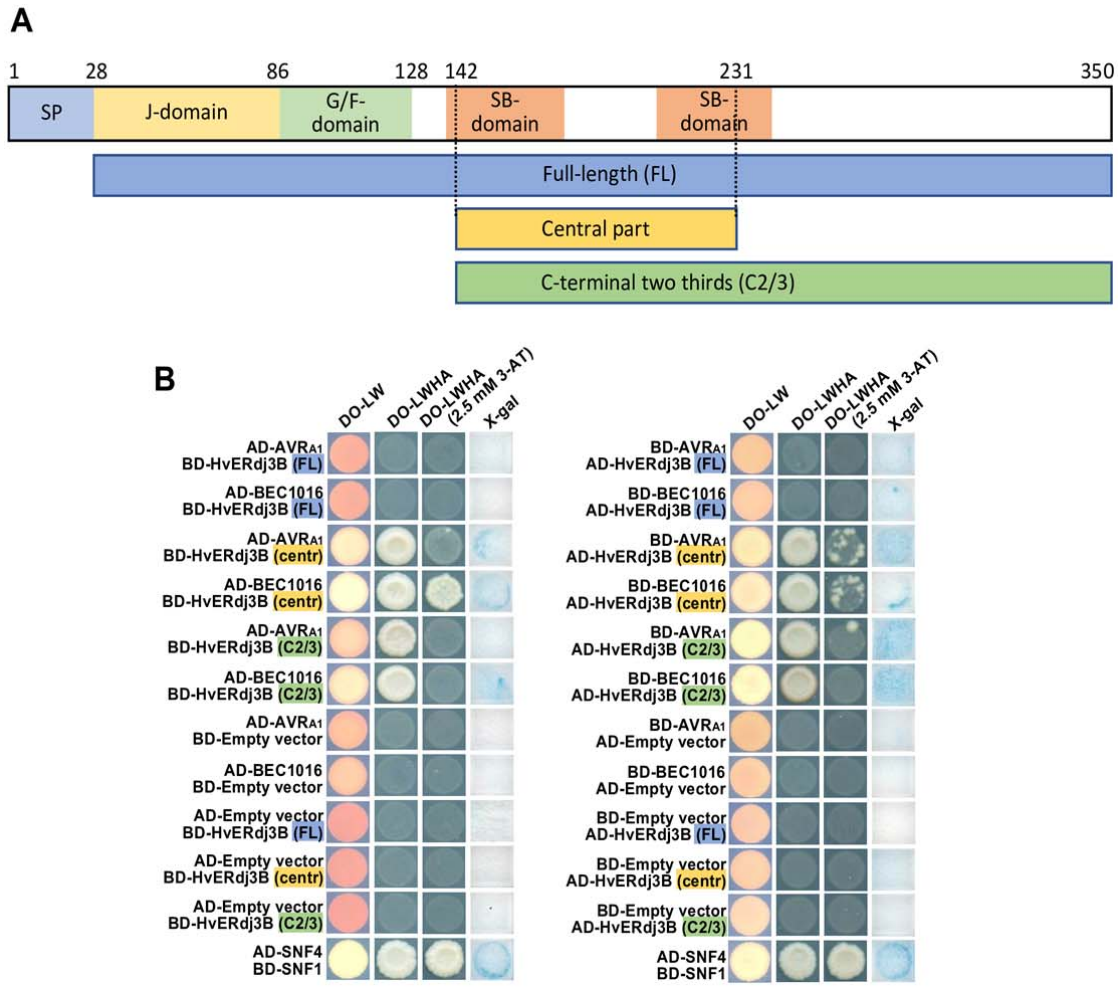

Figure 3. AVR_{A1} and BEC1016 interact with the central part of barley *Hv*ERdj3B in Y2H. A, The domains of the 350 aa *Hv*ERdj3B protein and the Y2H-fragments. The signal peptide (SP), the J-domain and the glycine/phenylalanine (G/F)-rich domain are indicated as well as the substrate binding domain predicted according to an alignment with the most closely related mammalian J-domain protein (Chen et al., 2017). Below the three Y2H-fragments are shown. **B,** Yeast transformed with the destination vectors pDEST-AS2-1 (GAL4 binding-domain (BD)) and pDEST-ACT2-1 (GAL4 activation-domain (AD)) (Robertson, 2004) in different combinations of domain-fusions to effectors and the full-length (FL), the central part (centr) and the C-terminal two-thirds (C2/3) of *Hv*ERdj3B. Growth on dropout (DO)-medium lacking leucine (L) and tryptophan (W) indicated presence of both constructs. Growth on DO-medium lacking L, W, histidine (H) and adenine (A) +/- 2.5 mM 3-amino-1,2,4-triazole (3AT) indicated protein-protein interaction. β-galactosidase assay (X-gal), also indicating protein-protein interaction, was performed on filter paper prints of DO-LW-grown yeast. SNF1/SNF4 was used as a positive control and empty vectors were used as negative control.

193 peptide) was used. GFP fluorescence signal was observed only when the *Hv*ERdj3B-cGFP fusion

Figure 4

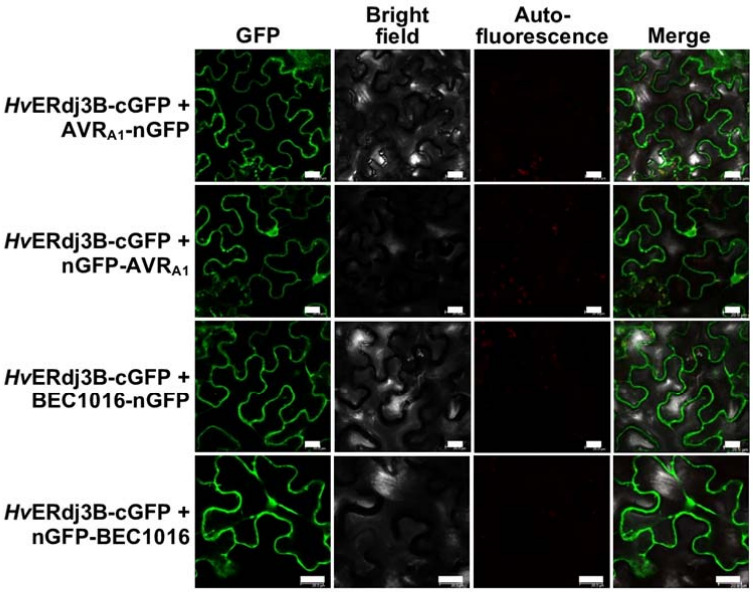

Figure 4. Interactions of *Hv*ERdj3B and AVR$_{A1}$ as well as BEC1016 in living plant cells confirmed by BiFC. Reconstitution of fluorescent GFP was observed in *N. benthamiana* epidermal cells expressing the shown combinations of the C and N-terminal parts of GFP fused with *Hv*ERdj3B (w/o SP) and AVR$_{A1}$/BEC1016 (w/o SP). The remaining combinations did not allow fluorescent GFP to reconstitute (see **Fig. S5**). Expression constructs were introduced using *Agrobacterium* infiltration, and epidermal cells were observed by laser scanning confocal microscopy 48 h later. Size bars, 20 μm.

194 was combined with nGFP fused to the N-terminal or the C-terminal of the effectors (**Figure 4**). No
195 GFP fluorescence was observed for any of the remaining six combinations for each effector
196 (**Supplemental Figure S5**), supporting the specificity of the interactions.
197 Taken together, these results confirmed that the central portion (aa 142-231) of the
198 J-domain protein *Hv*ERdj3B interacts with the diverged RALPH effectors AVR$_{A1}$ and BEC1016.
199 According to alignment with the most closely related mammalian J-domain protein this section

200 corresponds very well with the predicted substrate-binding domain (Chen et al., 2017). *In planta*,
201 however, this domain appears accessible for binding in the full-length *Hv*ERdj3B, which is a
202 prerequisite for the interaction to be functionally relevant.
203
204 **_Hv_ERdj3B is an ER luminal J-domain protein required for immunity during powdery mildew**
205 **attack**
206 *HvERdj3B* encodes a J-domain protein with an N-terminal signal peptide for ER targeting. The
207 mature protein has a high amino acid identity of 77% to its closest Arabidopsis homologue,
208 *At*ERdj3B, which is localized to the ER (Yamamoto et al., 2008). A strong accumulation of the
209 *HvERdj3B* transcript was observed during *Bgh* penetration, peaking at 20 h after inoculation
210 (**Supplemental Figure S2**), in line with an involvement in the immune response. Indeed, *At*ERdj3B
211 has previously been implicated in immunity in Arabidopsis, where it is required for triggering of
212 responses to the bacterial elongation factor-Tu (Nekrasov et al., 2009). To investigate whether
213 *Hv*ERdj3B contributes to the immunity to *Bgh*, we silenced the *HvERdj3B* gene in barley plants
214 using transient-induced gene silencing (TIGS). Two RNAi constructs were generated with different
215 *HvERdj3B* fragments and, together with a GUS reporter construct, bombarded into single
216 epidermal cells of leaves of one-week-old Golden Promise leaves. Two days later, the leaves were
217 inoculated with *Bgh* and formation of fungal haustoria was assessed after another 2 days. Our
218 data revealed that silencing of *HvERdj3B* significantly enhances the penetration rate, as *HvERdj3B*-
219 RNAi-1 and *HvERdj3B*-RNAi-2 on average tripled the number of haustoria (P value = 0.001). The
220 *Mlo* RNAi positive control reduced the number of haustoria by ~40% (**Figure 5A**). This increase in
221 the level of infection suggests that *Hv*ERdj3B plays an essential role in barley immunity.
222 To reveal *Hv*ERdj3B's subcellular localization, a C-terminal mYFP fusion of it (w. SP)
223 was expressed in epidermal cells of barley leaves. Laser scanning confocal microscopy indicated
224 that *Hv*ERdj3B is an ER protein as the mYFP signal has a reticulate pattern, which overlaps with the
225 SP-mCherry-HDEL ER marker (**Figure 5B**). This localization of *Hv*ERdj3B found in barley was
226 confirmed in *N. benthamiana* (**Supplemental Figure S6**). Next, we tested if *Hv*ERdj3B, as expected,
227 is an ER luminal protein. Here we made use of a split GFP system different from BiFC. GFP is barrel-
228 shaped and consists of 11 β-sheets (GFP1-11), which can be split into two fragments, β-sheets 1–
229 10 (GFP1-10) and β-sheet 11 (GFP11). The two parts of GFP have affinity for one-another, and

Figure 5

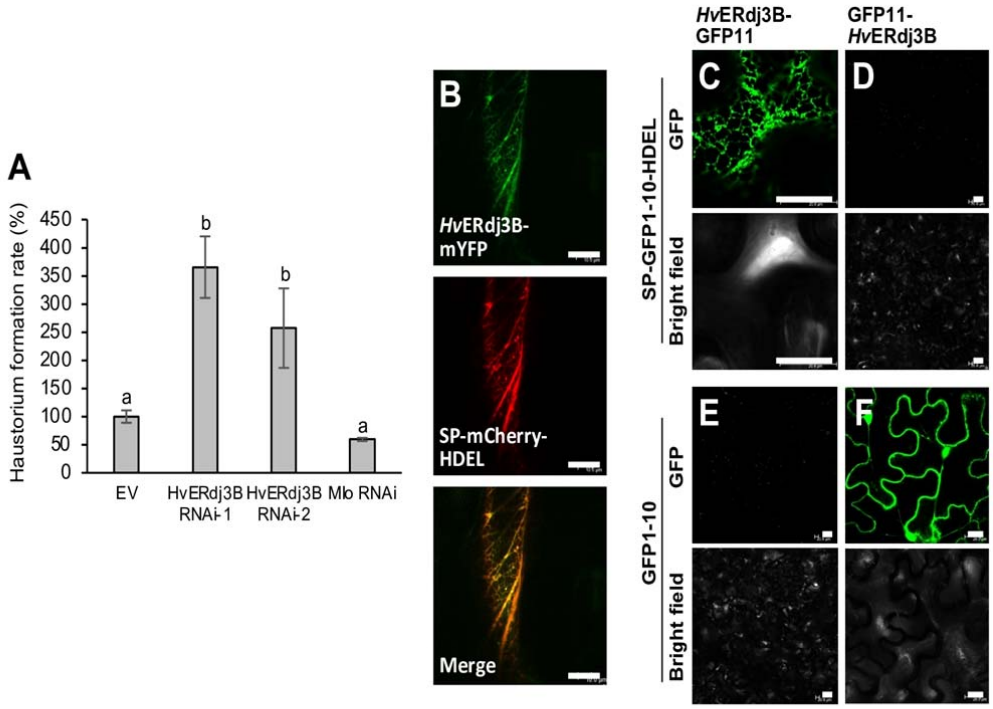

Figure 5. *Hv*ERdj3B is an ER luminal protein contributing to preinvasive immunity. A, One-week-old barley leaves, bombarded with RNAi and GUS reporter constructs, were inoculated with *Bgh* and scored for fungal haustorium formation, calculated as the ratio of haustoria-containing transformed cells (GUS expressing cells) divided by the total number of transformed cells. Data shown are mean values of four independent experiments. Error bars, SE. Letters (a and b) indicate significant differences calculated using a logistic regression model ($P < 0.001$). **B,** Localization of *Hv*ERdj3B in barley leaf epidermal cells. A ubiquitin promoter-driven expression construct encoding *Hv*ERdj3B (w. SP) fused to the N-terminus of mYFP was co-transformed with an SP-mCherry-HDEL construct into barley epidermal cells using particle bombardment. The cells were observed by confocal laser scanning microscopy 48 h later. **C-F,** Localization of *Hv*ERdj3B in *N. benthamiana* leaf epidermal cells using the split GFP system. *Hv*ERdj3B(w. SP)-GFP11 and SP-GFP1-10-HDEL reconstitute reticulate fluorescent GFP, while GFP11-*Hv*ERdj3B (w/o SP) and GFP1-10 reconstitute cytosolic and nuclear fluorescent GFP. Expression constructs were introduced using *Agrobacterium* infiltration, and epidermal cells were observed by laser scanning confocal microscopy 48 h later. Size bars, 20 μm (B,C,F) and 40 μm (D,E).

230 when they co-localize in the same compartment, a fluorescent GFP complex will be assembled (Xie

231 et al., 2017). This was visualized as a reticulate GFP signal when the *Hv*ERdj3B-GFP11 fusion
232 protein was co-expressed with an SP-GFP1-10-HDEL construct that delivers and retains GFP1-10 in
233 the ER lumen (**Figure 5C**). No visible signal appeared when *Hv*ERdj3B-GFP11 was co-expressed
234 with cytosolic GFP1-10 (**Figure 5E**). Furthermore, when GFP11-*Hv*ERdj3B without signal peptide
235 was co-expressed with either SP-GFP1-10-HDEL or with cytosolic GFP1-10, GFP signal was absent
236 and present, respectively (**Figure 5D,F**). In summary, these results show that *Hv*ERdj3B is
237 important for barley immunity to *Bgh* and that it is located inside the ER lumen. This complements
238 accumulating evidence of the role of ERQC and ERdj3B in plant immunity (Nekrasov et al., 2009;
239 Tintor and Saijo, 2014).
240
241 **AVR_{A1} and BEC1016 translocate from the plant cytosol to the ER lumen by unknown**
242 **mechanism(s)**
243 For interactions to occur between either AVR_{A1} or BEC1016, and *Hv*ERdj3B in barley epidermal
244 cells attacked by *Bgh*, the two effectors are required to translocate from the fungus across either
245 the plant plasma membrane or the extrahaustorial membrane into the plant cytosol; and then
246 further across the plant ER membrane and into the ER lumen. Indirect evidence that AVR_{A1}
247 translocates into the plant epidermal cell cytosol comes from the observation that it functions as
248 an avirulence protein that binds to the cytosolic R-protein, MLA1, and triggers a hypersensitive
249 response (HR) (Lu et al., 2016). It is assumed that BEC1016 also enters the plant epidermal cell,
250 since the number of haustoria is increased when this effector is expressed in the epidermal cell
251 cytosol after particle bombardment (Fig. 1A). To inquire whether both can translocate across the
252 ER membrane, we started by over-expressing AVR_{A1}-GFP and BEC1016-GFP (both w/o signal
253 peptide) in *N. benthamiana* epidermal cells. Here they were both localized to the cytosol and
254 nucleus together with free mCherry, and no obvious ER signal could be distinguished as there was
255 a complete overlap between the GFP and mCherry fluorescent signals (**Figure 6**). Expression in
256 barley epidermal cells also suggested the effectors mainly to be cytosolic (**Supplemental Figure**
257 **S7**).
258 However, to interact with *Hv*ERdj3B, the two effectors will have to enter the plant
259 ER. To test this more rigorously, we again used our split GFP system (Xie et al., 2017). We
260 generated constructs for fusing GFP11 to both the N and C-terminus of AVR_{A1}, BEC1016 and

Figure 6

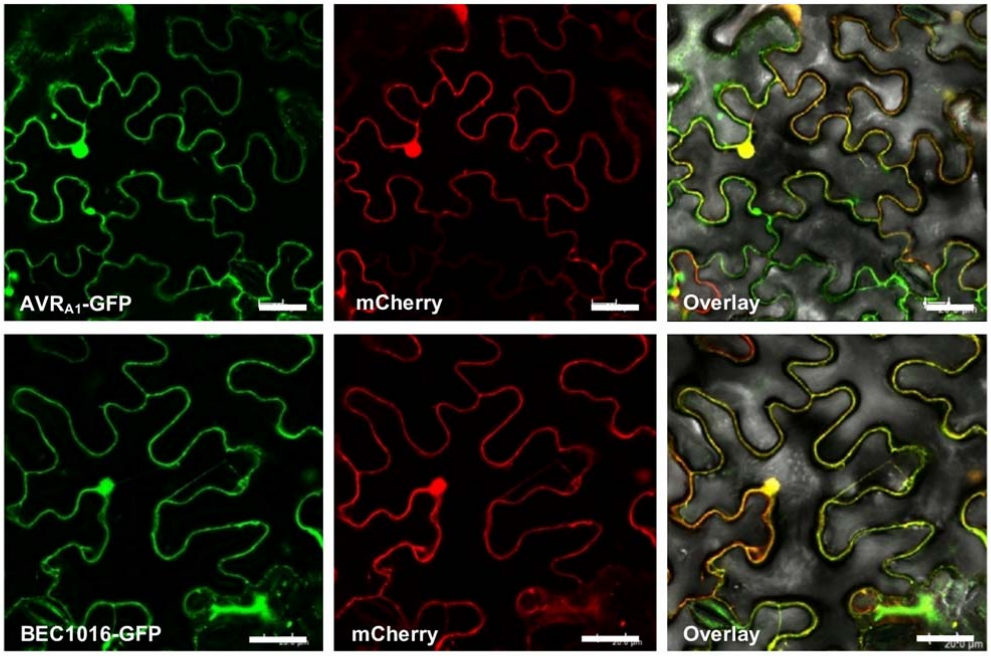

Figure 6. AVR$_{A1}$ and BEC1016 localized in the cytosol and nucleus of *N. benthamiana* epidermal cells. Constructs for expression of effectors (w/o SP) were introduced using *Agrobacterium* infiltration, and epidermal cells were observed by laser scanning confocal microscopy 48 h later. Size bars, 40 μm.

261 CSEP0105, all w/o SP. CSEP0105, which interacts with small heat shock proteins (Ahmed et al.,
262 2015), was used as a negative control. These were then co-expressed with constructs for cytosolic
263 GFP1-10 and ER-luminal SP-GFP1-10-HDEL in all combinations (**Figure 7**). GFP11 fused to the N and
264 C-terminal of CNX^{TM}, the transmembrane domain of the ER membrane protein, calnexin 1 (Xie et
265 al., 2017), was used as reference (**Figure 7A,B,I,J**). All three effectors combined with GFP1-10
266 resulted in cytosolic and nuclear GFP signal (**Figure 7C-H**). Yet, all combinations of AVR$_{A1}$ and
267 BEC1016 with SP-GFP1-10-HDEL in addition resulted in cells with distinct GFP signal from a

Figure 7

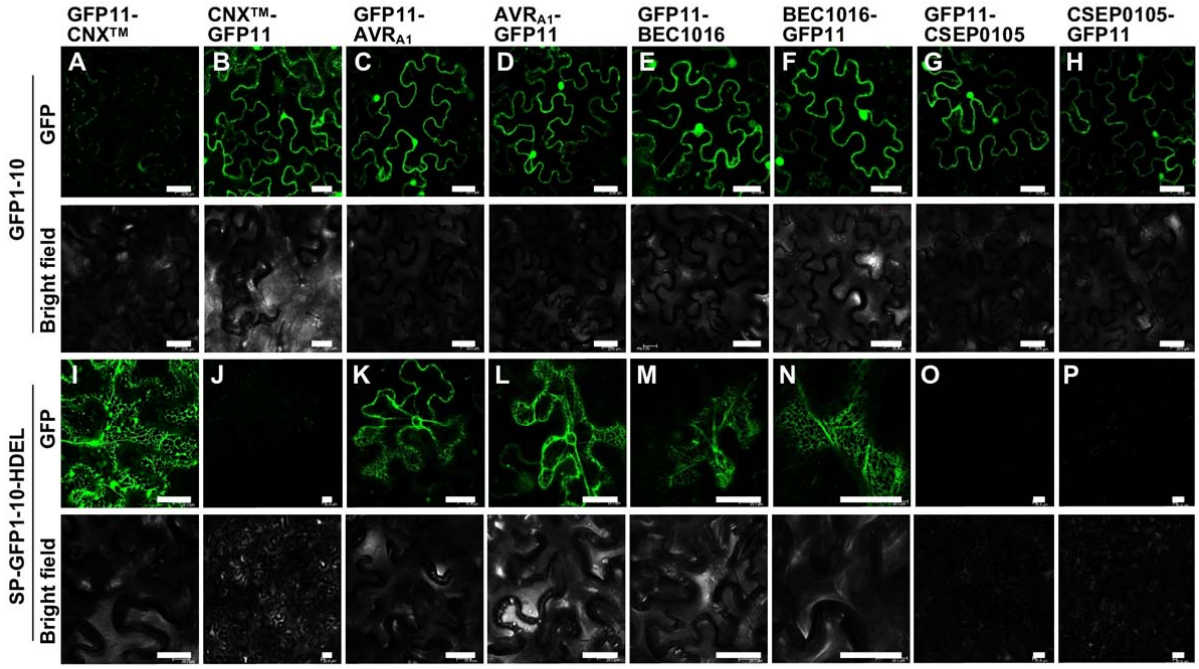

Figure 7. AVR$_{A1}$ and BEC1016 are partially translocated into the ER lumen. The GFP1-10/GFP11 self-constituting fluorescence protein demonstrates cytosolic and ER-luminal protein localizations *N. benthamiana* epidermal cells. **A-B and I-J,** GFP11-CNX^{TM} and CNX^{TM}-GFP11 confirm SP-GFP11-HDEL to be ER-luminal and GFP1-10 to be cytosolic, respectively. **C-H and K-P,** AVR$_{A1}$, BEC1016 and CSEP0105 (all w/o SP) are cytosolic while AVR$_{A1}$ and BEC1016 (both w/o SP) are also ER-lumunal, indicated by their reticulate and perinuclear signals (see also **Fig. S8**). Expression constructs were introduced using *Agrobacterium* infiltration, and epidermal cells were observed by laser scanning confocal microscopy 48 h later. Size bars, 40 μm.

268 reticulate network and the perinuclear space (**Figure 7K-N, Supplemental Figure S8**). Since this
269 was never seen for CSEP0105 (**Figure 7O,P**) and since the ER-localized GFP11-CNX^{TM}/SP-GFP1-10-
270 HDEL combination also gave reticulate network signal (**Figure 7I**), the data indicate that a fraction
271 of the cytosolic AVR$_{A1}$ and BEC1016 specifically translocate into the ER lumen post-translationally
272 and independently of their signal peptides.
273
274

275 **DISCUSSION**

276 Powdery mildew fungi are obligate biotrophic pathogens that feed on living plant tissues for
277 nutrient uptake via haustoria. To suppress host defenses and promote colonization, these
278 pathogens deliver a large repertoire of effectors into host cells (Frantzeskakis et al., 2018).
279 Therefore, identifying the host targets of these effectors and their function will lead to detailed
280 understanding of how infection is established and maintained. We focused on *Bgh* AVR_{A1} and
281 BEC1016, as examples of avirulence proteins and proteins having a detectable contribution to
282 fungal virulence, respectively (Lu et al., 2016; Pliego et al., 2013). Here we found that bacterial
283 T3SS-based delivery of these effectors reduced defense-associated callose deposition and that
284 over-expression enhanced *Bgh* haustorial development. Through Y2H-NGIS, these effectors were
285 found to target the same host protein, *Hv*ERdj3B, which we further substantiated through binary
286 Y2H and BiFC assays. Silencing of the *HvERdj3B* gene in barley led to increased formation of *Bgh*
287 haustoria, indicating that this ER protein is involved in the plant's immunity against fungal
288 penetration.

289 It is well-documented that ER stress responses and ERQC contribute to plant
290 immunity in several ways. Our data are consistent with a previous study showing that a T-DNA line
291 mutated in *HvERdj3B*'s closest homologue in *Arabidopsis*, *AtERdj3B*, is more susceptible to
292 bacterial pathogens (Nekrasov et al., 2009). Here it was reported that *At*ERdj3B is involved in PTI.
293 In the ER, it forms a complex with SDF2 and the Hsp70 BiP1, which are required for proper
294 trafficking and function of the plasma membrane leucine-rich-repeat receptor kinases, EFR.
295 *Hv*ERdj3B may have a similar function and may be involved in proper functioning of PRRs in barley.
296

297 Besides being required for processing of pattern-recognition receptors, ERQC is required for
298 secretion of antimicrobial proteins and linked to pathogen-induced programmed cell death (Li et
299 al., 2009; Moreno et al., 2012; Qiang et al., 2012; Kørner et al., 2015). In addition, a recent study
300 showed that the ER proteins, UBAC2 and PICC, interact with each other and are required for
301 proper delivery of callose synthase to the plasma membrane and for flagellin-triggered callose
302 deposition (Wang et al., 2019). As callose is important for immunity towards penetration by
303 powdery mildew fungi (Voigt, 2016), it will be interesting to see if future studies can demonstrate
304 that the ERdj3B/BiP complex is required for UBAC2/PICC-dependent callose deposition. Therefore,

305 even if ERdj3B is essential for maturation of certain PRRs in the ER, there might be additional ways
306 by which it contributes to plant immunity and thus how *Bgh* uses AVR_{A1} and BEC1016 to aid the
307 penetration process.

308 Since our immediate localization study suggested both effectors to be cytosolic and
309 nuclear, while *Hv*ERdj3B was found to be ER-luminal, we used the split GFP system to demonstrate
310 that these effectors are also translocated into the ER. There are other studies showing that
311 pathogen effectors enter the ER to facilitate infection by targeting ER-localized host proteins. For
312 instance, the RXLR effector PcAvr3a12 from the *Arabidopsis* pathogen, *Phytophthora capsici*, can
313 post-translationally enter the ER and target the ER-localized host PPIase, FKBP15-2, which is
314 involved in ER stress-sensing and required for ER stress-mediated plant immunity (Fan et al.,
315 2018). Furthermore, it has been reported that an essential effector, PsAvh262, secreted by the
316 soybean pathogen, *P. sojae*, translocates from the host cytosol into the ER to stabilize BiPs,
317 thereby suppressing ER stress-triggered cell death and facilitating infection (Jing et al., 2016). In
318 both cases, it was shown by BiFC that effector-target interactions occur inside the ER. Yet another
319 recent study showed that a nematode effector (CLE) is translocated from the plant cell cytosol to
320 the ER, and then secreted as an extracellular receptor ligand (Wang et al., 2021). Here post-
321 translational ER uptake was demonstrated using the GFP1-10/11 system, which we also used.
322 Together these observations suggest that these effectors hijack one or more signal peptide-
323 independent plant ER uptake mechanisms.

324 AVR_{A1} and BEC1016 both interact with *Hv*ERdj3B and both enter the ER post-
325 translationally and signal peptide-independently. Yet they have very diverse amino acid
326 sequences. However, the two effectors appear derived from an ancient RNAse, and they are
327 potentially structurally related (Pedersen et al., 2012), which may explain the shared functions.
328 Interestingly, the ERQC machinery is known to engage in the post-translational ER protein uptake
329 through the Sec61 translocon complex (Zimmermann et al., 2021). Thus, we consider that
330 interactions of AVR_{A1} and BEC1016 with *Hv*ERdj3B may facilitate one-way movement through this
331 translocon into the ER lumen. Previously, we found that silencing of the barley Sec61 β- and γ-
332 subunits both reduce the plant's susceptibility to *Bgh* (Zhang et al., 2013; Xu et al., 2015). These
333 findings were difficult to explain as preventing ER uptake of immunity-associated proteins, such as
334 PR-proteins and PM-bound PRR should increase the plant susceptibility. However, our present

335 finding of a susceptibility suppressing role AVR_{A1} and BEC1016 (Fig. 1), which both enter the ER,
336 may make the consequences of Sec61 (Zhang et al., 2013; Xu et al., 2015) more meaningful.
337 Often effectors are recognized indirectly by NLRs after they have impacted effector
338 targets, which are guarded and associated with the NLRs (Carter et al., 2019; Ngou et al., 2022;
339 Thordal-Christensen, 2020). However, an effector target that contributes to immunity, like
340 *Hv*ERdj3B, inside the ER may not be guarded by an NLR, as to date, such receptors have not been
341 localized in this compartment. Instead, this favors a requirement for direct effector monitoring by
342 NLRs in the cytosol, which agrees with the direct recognition and interaction of AVR_{A1} and the NLR,
343 MLA1 (Lu et al., 2016). One may speculate whether targeting an ER luminal host protein thus has
344 provided an evolutionary benefit to the pathogen, since it may be more demanding for the plant
345 to invent specific recognition of each effector, rather than guarding proteins targeted by more
346 effectors potentially from different pathogens.
347
348 **MATERIAL AND METHODS**
349 **Plant and Fungal Materials**
350 Seedlings of barley (*Hordeum vulgare* L.) cv. 'Golden Promise' were grown at 16 h light (150 µE s^{-1}
351 m^{-2}, 20°C) / 8 h of darkness (20°C) to be used for inoculations, gene amplifications, transient-
352 induced gene silencing (TIGS), overexpression, and callose deposition assays after effector-delivery
353 using EtHAn. *Blumeria graminis* f. sp. *hordei* (*Bgh*) isolate C15 was propagated on barley P-02
354 plants in a cycle of 1 week. Four to six-week-old *Nicotiana benthamiana* plants were used for BiFC
355 and subcellular localization studies after Agrobacterium-mediated leaf cell transformation.
356
357 **Gateway Plasmid Construction**
358 Coding DNA sequences (CDS) for the effectors, AVR_{A1} and BEC1016, w/o their signal peptides,
359 were amplified using primer pairs listed in **Supplemental Table S2**. PCR was performed on cDNA
360 from barley leaves infected with *Bgh*, and the fragments were cloned into pENTR/D-TOPO®
361 vectors (Invitrogen), with or without stop codons. The CDS for the full-length barley *Hv*ERdj3B
362 (HORVU1Hr1G022990) with stop codon was synthesized by TWIST Bioscience (San Francisco, CA,
363 USA). Fragments of *Hv*ERdj3B were amplified therefrom using primers listed **Supplemental Table**
364 **S2** and cloned into pENTR/D-TOPO. Subsequently, the entry clone inserts were transferred to

365 destination vectors using Gateway LR cloning reactions (Invitrogen). RNAi constructs were
366 generated in the 35S promoter-driven hairpin destination vector, pIPKTA30N (Douchkov et al.,
367 2005). The *Hv*ERdj3B-RNAi-1 and -2 constructs contain *Hv*ERdj3B CDS fragments from positions
368 283 to 579 and 532 to 879, respectively. These sequences were predicted using the si-Fi open-
369 source software (Lück et al., 2019). For over-expression constructs, the CDSs for *Hv*ERdj3B (with
370 signal peptide), AVR_{A1} and BEC1016 (w/o signal peptides) were transferred into pUbi-mYFP-GW-
371 Nos and pUbi-GW-Nos destination vectors. All the constructs were sequenced for confirmation.
372
373 **Barley Single Cell Transient-Induced Gene Silencing and Over-Expression**
374 Barley leaf epidermal cell transformation was obtained after particle bombardment as described
375 by Douchkov et al. (2005) and Nowara et al. (2010), using the biolistic PDS-1000/He Particle
376 Delivery System from Bio-Rad. For each bombardment, six detached 1st leaves of one-week-old
377 Golden Promise barley plants were used. The particle coating was performed using 7 µg of DNA
378 for each construct together with 2.4 mg of gold, 1 µg $µl^{-1}$ of protamine (Sivamani et al, 2009) and
379 0.625 M $CaCl_2$ (Rasco-Gaunt et al., 1999). For the bombardments, a hepta adapter and rupture
380 discs bursting at a helium pressure of 1.100 psi were used. After bombardment, the leaves were
381 transferred onto 1% phytoagar petri dishes containing 40 mg ml^{-1} benzimidazole. For TIGS, the
382 constructs were co-transformed with a GUS reporter gene construct driven by the pUbi promoter
383 into the epidermal cells. Two days later, the leaves were inoculated with *Bgh*, and after another 2
384 days, they were stained for GUS activity. Transformed (blue) cells were assessed microscopically
385 for the presence of haustoria as an indication of fungal infection. The haustorium formation rate
386 was calculated as the number of blue cells with haustoria divided by the total number of blue cells.
387 An mYFP and the empty vector pIPKTA30N were used as negative controls and the Mlo RNAi
388 (pIPKTA36) (Douchkov et al., 2005) construct was used as positive control. The effect of constructs
389 was analysed by a logistic regression model with random effects, assuming a binominal
390 distribution, with construct as fixed effect and the experiment × construct × leaf interaction as
391 random effect. The analyses were performed in PC-SAS (release 9.4, SAS Institute, Cary, NC). The
392 SP-mCherry-HDEL construct was from Nelson et al. (2007).
393

394 ***Agrobacterium tumefaciens* infiltration-mediated transformation of *Nicotiana benthamiana* leaf**
395 **cells**
396 T-DNA construct were introduced into *A. tumefaciens* strain GV3101 by electroporation. The
397 transformed bacterial cells were grown on LB agar plates supplemented with Rifampicin,
398 Spectinomycin and Gentamycin antibiotics. For leaf cell transformation, over-night liquid cultures
399 (28°C) of recombinant *A. tumefaciens* were harvested by centrifugation and resuspended in 10
400 mM $MgCl_2$, 10 mM MES and 200 µM acetosyringone to OD_{600}=0.6. A strain of *A. tumefaciens* with
401 a construct expressing the p19 silencing suppressor (Voinnet et al., 2003) was managed the same
402 way. The resuspended *A. tumefaciens* transformants, including the one with the P19 construct,
403 were mixed in equal ratios and infiltrated into leaves of four to six-week-old *N. benthamiana*.
404
405 **Yeast 2-Hybrid, Next-Generation-Interaction Screen**
406 The *Bgh* effectors AVR_{A1} and BEC1016 were used as baits in Y2H-NGIS to mine for novel protein
407 interactions. Bait sequences (w/o signal peptides) were fused with the GAL4 transcription factor
408 binding domain (GAL4-BD) in the p97-BD, Leu2p vector and transformed into *Saccharomyces*
409 *cerevisiae* strain Y8930 (Dreze et al., 2010). Pooled mRNA from an infection time course of the
410 resistant barley line CI 16151 (*Mla6*) and four fast-neutron-derived mutants inoculated with *Bgh*
411 isolate 5874 (AVR_{a1}, AVR_{a6}) (Surana, 2017; Chapman et al. 2021), was used to prepare a three-
412 frame cDNA prey library in the Gateway-compatible ARS4/CEN6 GAL4 activation domain (AD)
413 vector, p86-AD, Trp1p (Dreze et al. 2010; Yu et al. 2015). After transforming the library into *S.*
414 *cerevisiae* strain Y8800, 1.1 x 10^7 primary clones were mated with each bait clone and
415 subsequently cultured in three replicates under two conditions (selection and non-selection). At
416 the end of each culture, prey plasmids were isolated, and the prey cDNA fragments were amplified
417 by PCR. Amplicons were sent for sequence analysis using the Illumina HiSeq 2500 platform at the
418 Iowa State University sequencing facility, collecting 5–10 million reads per sample. Y2H-NGIS data
419 from these experiments were analyzed using the NGPINT and Y2H-SCORES software (Banerjee et
420 al., 2021; Velásquez-Zapata et al., 2021) to reconstruct the prey fragments and rank them as
421 interactors of each bait. Outputs from these pipelines allowed us to identify interacting prey
422 fragments, their frame with the Gal4-AD as well as enrichment and specificity scores that assess
423 their properties as Y2H interactors.

424

425 **Binary Yeast 2-Hybrid Assay**

426 Using the output from the Y2H-NGIS, we designed primers to re-clone identified prey fragments
427 into p86-AD to confirm interactions using binary Y2H (Dreze et al., 2010) under three levels of
428 selective media: Diploid selection (SC-LW), interaction selection (SC-LWH) and specific selection
429 (SC-LWH + 0.1 mM 3-AT) using three dilutions (10^0, 10^{-1}, 10^{-2}) as shown in **Supplemental Figure S4**.
430 After the first confirmation of *Hv*ERdj3B as prey, new AVR_{A1}, BEC1016 and *Hv*ERdj3B constructs
431 were made in the destination vectors pDEST-AS2-1 (GAL4-BD) and pDEST-ACT2-1 (GAL4-AD)
432 (Robertson, 2004). These constructs were transformed into the haploid yeast strains, Y189 and
433 Y190, respectively. Subsequent matings, selections and *LacZ* reporter assays were made according
434 to the Matchmaker Gold Yeast Two-Hybrid System user manual (Clontech; Mountain View, Ca,
435 USA).

436

437 **Bimolecular Fluorescence Complementation Assay**

438 The CDS for full-length barley *Hv*ERdj3B and both effectors, w/o signal peptides, and with and w/o
439 stop codons, were transferred to 35S promoter-driven BiFC binary destination vectors (Kamigaki et
440 al. (2016) as N- and C-terminal fusions of nGFP (aa 1 to 174) and cGFP (aa 175 to 239). Two-by-two
441 combinations of constructs were transformed into *N. benthamiana* leaves by *A. tumefaciens*
442 infiltration. Two days after infiltration, the fluorescence signals of all eight possible
443 AVR_{A1}/*Hv*ERdj3B combinations and of all eight possible BEC1016/*Hv*ERdj3B combinations were
444 evaluated by a laser scanning confocal microscopy.

445

446 **Localization of Effectors in the ER**

447 The GFP1-10/GFP11 split GFP system (Xie et al., 2017) was used to document presence of
448 effectors in the ER lumen. CDS for the effectors AVR_{A1} and BEC1016, w/o their signal peptides,
449 were transferred to the T-DNA Gateway destination vectors, pGFP11-GW and pGW-GFP11, to fuse
450 them to GFP11. T-DNA constructs for GFP11-CNX^{TM} and CNX^{TM}-GFP11 were from Xie et al. (2017).
451 These were co-expressed with constructs for cytosolic GFP1-10 and ER-luminal SP-GFP1-10-HDEL
452 from Xie et al. (2017).

453

454 **Callose Deposition Assay**

455 CDSs for the GUS reporter gene and both CSEPs, w/o signal peptides and with stop codons were
456 transferred to the AvrRPS4 promoter-driven destination vector, pEDV6 (Fabro et al., 2011), and
457 transformed into *Pseudomonas fluorescens* EtHAn (Thomas et al., 2009) by electroporation.
458 Transformed EtHAn strains were grown over-night in King's B medium containing ampicillin,
459 chloramphenicol, tetracycline and gentamicin at 28°C. The bacteria were harvested by
460 centrifugation and resuspended in 10 mM $MgCl_2$ to a final OD_{600}=0.3 and infiltrated into leaves of
461 eight-day-old barley. Twenty-four hours later, the callose response was assayed in the infiltrated
462 leaf areas by aniline blue fluorescence using a Nikon ECLIPSE Ni-U fluorescence microscope. For
463 one repeat, ten 1110 μm x 740 μm (5184 × 3456 pixels) images from random sites at one leaf
464 were used to quantify the number of callose deposits and the accumulated area of callose
465 deposits using the Fiji open-source platform (Schindelin et al., 2012, Jin and Mackey, 2017). The
466 outcomes of effectors were calculated relative to GUS as control and analysis of the callose
467 deposition data was performed for the total number and area of the callose deposits
468 independently. We performed a repeated measures ANOVA (Keselman et al., 2001) to test the
469 effect of the treatments considering the repeated measures by leaf. Significant treatments effects
470 were further explored with a paired-sample t test and the *P* values were adjusted using the
471 method of Benjamini and Hochberg (1995).

472

473 **Differential transcript accumulation**

474 RNA-Seq data were extracted from an infection time course of barley CI 16151 and the derived
475 fast-neutron mutant, *mla6*-m18982, at 0, 16, 20, 24, 32, and 48 hours after inoculation with *Bgh*
476 isolate 5874 (AVR_{a1}, AVR_{a6}) (5 genotypes × 6 time points × 3 biological replications; NCBI-GEO
477 GSE101304) and analyzed as described in (Chapman et al., 2021; Hunt et al., 2019). Genes were
478 differentially expressed at an adjusted *P* of < 0.001 for barley and < 0.003 for *Bgh* were considered
479 significant.

480

481 **Availability of Y2H-NGIS code, data, and materials**

482 Infection-time-course RNA-Seq data are at NCBI-GEO under the accession number GSE101304
483 (https://www.ncbi.nlm.nih.gov/gds/?term=GSE101304). R code and the ReadMe file for the

484 NGPINT and Y2H-SCORES software used to identify *Bgh* AVR_{A1} and BEC1016 interactors are
485 provided at the GitHub page (https://github.com/Wiselab2/). Raw Y2H-Seq reads are at NCBI-GEO
486 under accession numbers GSE164954 (AVR_{A1}/CSEP0008) and GSE166108 (BEC1016/CSEP0491).

487

488 **The following supplementary material is available:**

489 **Supplemental Figure S1.** Attempted alignment of the amino acid sequences of AVR_{A1} (CSEP0008,
490 BLGH_03023) and BEC1016 (CSEP0491, BLGH_07006).

491 **Supplemental Figure S2.** Transcript accumulation on barley inoculated with *Bgh* isolate 5874.

492 **Supplemental Figure S3.** EtHAn-delivery of β-glucuronidase into barley leaf cells.

493 **Supplemental Figure S4.** Y2H used to validate interactions between AVR_{A1}, BEC1016 and *Hv*ERdj3B

494 **Supplemental Figure S5.** Bimolecular fluorescence complementation study of the interaction
495 between AVR_{A1}, BEC1016 and *Hv*ERdj3B.

496 **Supplemental Figure S6.** Subcellular localization of *Hv*ERdj3B in *N. benthamiana* epidermal cells.

497 **Supplemental Figure S7.** Localization of AVR_{A1} and BEC1016 in barley leaf epidermal cells.

498 **Supplemental Figure S8.** BEC1016 can translocate into the ER.

499 **Supplemental Table S1.** Y2H-SCORES for the AVRA1 and BEC1016 baits.

500 **Supplemental Table S2.** Primer sequences for plasmid constructions (5´ to 3´)

501

502 **ACKNOWLEDGMENTS**

503 We thank the late Dr. Patrick Schweizer (Leibniz Institute of Plant Genetics and Crop Plant
504 Research, Gatersleben, Germany) for providing the RNAi vector and the Mlo RNAi construct, Dr.
505 Masumi Robertson (Commonwealth Scientific and Individual Research Organization Plant Industry)
506 for the Gateway Y2H vectors (pDEST-ACT2 and pDEST-AS2-1), Greg Fuerst (USDA-ARS at Iowa State
507 University) for conducting the *Bgh* time-course infection experiment and expert isolation of RNA
508 for the 3-frame Y2H library, Associate Professor Shoi Mano for the BiFC-vectors, and Drs. Pietro
509 Spanu (Imperial College, U.K.) and Ralph Panstruga (RWTH Aachen, Germany) for CSEP clones.
510 Research supported in part by China Scholarship Council for PhD-student scholarship
511 201708340064 to ZZ, Novo Nordisk Foundation Challenge grant NNF19OC0056457 to HTC, Villum
512 Fonden Experiment Programme grant 00028131 to HTC, Fulbright - Minciencias 2015 &
513 Schlumberger Faculty for the Future fellowships to VVZ, USDA-ARS Postdoctoral Research

514 Associateship and USDA-NIFA-ELI Postdoctoral Fellowship 2017-67012-26086 to JME, Oak Ridge
515 Institute for Science and Education under U.S. Department of Energy contract number DE-
516 SC0014664 to SB, and National Science Foundation - Plant Genome Research Program grant 13-
517 39348, USDA-National Institute of Food and Agriculture grant 2020-67013-31184 and USDA-
518 Agricultural Research Service project 3625-21000-067-00D to RPW. The funders had no role in
519 study design, data collection and analysis, decision to publish, or preparation of the manuscript.
520 Mention of trade names or commercial products in this publication is solely for the purpose of
521 providing specific information and does not imply recommendation or endorsement by the CSC,
522 NNF, VF, USDA, NIFA, ARS, DOE, ORAU/ORISE or NSF. USDA is an equal opportunity provider and
523 employer.
524
525 **Author contributions**
526 ZL: Transient effector OE and haustorial formation rate, extensive binary Y2H, protein
527 subcellular localizations, contributed to writing
528 VVZ: Y2H-NGIS, developed the Y2H-SCORES software to rank high-priority candidates, identified
529 *Hv*ERdj3B, and validated by first binary Y2H, contributed to statistics, contributed to writing,
530 JME: Initiated the overall concept and experimental plan. Constructed the 3-frame
531 barley/Blumeria Y2H library and developed Y2H-NGIS screen.
532 XL: Callose response to EtHAn infiltrations
533 WX: Assisted and supervised subcellular localizations
534 SB: Developed the NGPINT software and analyzed sequence count data.
535 HJLJ: Contributed to statistics
536 CP: Supervised and contributed to writing
537 RPW: Initiated the overall concept and experimental plan, organized, supervised and
538 contributed to writing
539 HTC: Organized and supervised the work, wrote first draft, lead the writing and finalized the
540 work
541
542
543 **Figure and table legends**
544
545 **Figure 1. Influence of AVR_{A1} and BEC1016 on *Bgh* infection and callose deposition in barley. A,**
546 Effect of transient over-expression of AVR_{A1} and BEC1016 on *Bgh* invasion. pUbi promoter-driven
547 over-expression constructs were co-bombarded with a GUS-reporter constructs into leaf
548 epidermal cells of 1-week-old barley and 2 days later inoculated with *Bgh*. After another 2 days,
549 the fungal haustorium formation was scored in GUS expressing cells. Data shown are mean values

550 of three independent experiments. Error bars, SE. Letters (a, ab and b) indicate significant
551 differences calculated using a logistic regression model (P = 0.0179). **B,** AVR_{A1} and BEC1016 can
552 reduce bacterium-triggered callose deposition in barley plants estimated as numbers of callose
553 spots (left) and area of callose spots (right). Leaves of eight-day-old barley plants were infiltrated
554 with EtHAn, transformed with pEDV6-GUS, pEDV6-AVR_{A1} or pEDV6-BEC1016, and 24 h later the
555 callose deposition we scored. Boxplots for the total number and total area of callose depositions
556 show data for all pictures taken across biological replicates (one replicate = ten pictures from each
557 of three leaves, ie. 30 pictures) under each treatment. A repeated measures ANOVA followed for a
558 paired sample t test were used to compare the treatments. ***, $P < 2x10^{-16}$. Data shown are based
559 on five independent experiments, statistically treated as replicates.
560
561 **Figure 2. Y2H-NGIS used to identify interactions between AVR_{A1}, BEC1016 and *Hv*ERdj3B. A,**
562 *Hv*ERdj3B gene model with exons depicted as blue boxes and introns as hash marks. **B,** Integrative
563 genomic view (IGV) obtained from the software NGPINT after Y2H-NGIS analysis of the *Hv*ERdj3B
564 prey reads selected by both the AVR_{A1} and the BEC1016 bait. Prey fragments were reconstructed
565 from the reads mapped to the *HvERdj3B* gene (shown in grey across the exons) in each Y2H-NGIS
566 dataset and located towards the 3' end of the gene in both cases. **C,** Expanded view of the 5'
567 fusion reads that allowed the determination of the frame and nucleotide-resolved prey fragments.
568 The fusion reads contain a prey plasmid sequence (shown in different colors as mismatches from
569 the reference gene) and the prey sequence.
570
571 **Figure 3. AVR_{A1} and BEC1016 interact with the central part of barley *Hv*ERdj3B in Y2H**. **A,** The
572 domains of the 350 aa *Hv*ERdj3B protein and the Y2H-fragments. The signal peptide (SP), the J-
573 domain and the glycine/phenylalanine (G/F)-rich domain are indicated as well as the substrate
574 binding domain predicted according to an alignment with the most closely related mammalian J-
575 domain protein (Chen et al., 2017). Below the three Y2H-fragments are shown. **B,** Yeast
576 transformed with the destination vectors pDEST-AS2-1 (GAL4 binding-domain (BD)) and pDEST-
577 ACT2-1 (GAL4 activation-domain (AD)) (Robertson, 2004) in different combinations of domain-
578 fusions to effectors and the full-length (FL), the central part (centr) and the C-terminal two-thirds
579 (C2/3) of *Hv*ERdj3B. Growth on dropout (DO)-medium lacking leucine (L) and tryptophan (W)

580 indicated presence of both constructs. Growth on DO-medium lacking L, W, histidine (H) and
581 adenine (A) +/- 2.5 mM 3-amino-1,2,4-triazole (3AT) indicated protein-protein interaction. β-
582 galactosidase assay (X-gal), also indicating protein-protein interaction, was performed on filter
583 paper prints of DO-LW-grown yeast. SNF1/SNF4 was used as a positive control and empty vectors
584 were used as negative control.
585
586 **Figure 4. Interactions of *Hv*ERdj3B and AVR_{A1} as well as BEC1016 in living plant cells confirmed**
587 **by BiFC.** Reconstitution of fluorescent GFP was observed in *N. benthamiana* epidermal cells
588 expressing the shown combinations of the C and N-terminal parts of GFP fused with *Hv*ERdj3B
589 (w/o SP) and AVR_{A1}/BEC1016 (w/o SP). The remaining combinations did not allow fluorescent GFP
590 to reconstitute (see **Fig. S5**). Expression constructs were introduced using *Agrobacterium*
591 infiltration, and epidermal cells were observed by laser scanning confocal microscopy 48 h later.
592 Size bars, 20 μm.
593
594 **Figure 5. *Hv*ERdj3B is an ER luminal protein contributing to preinvasive immunity. A,** One-week-
595 old barley leaves, bombarded with RNAi and GUS reporter constructs, were inoculated with *Bgh*
596 and scored for fungal haustorium formation, calculated as the ratio of haustoria-containing
597 transformed cells (GUS expressing cells) divided by the total number of transformed cells. Data
598 shown are mean values of four independent experiments. Error bars, SE. Letters (a and b) indicate
599 significant differences calculated using a logistic regression model ($P < 0.001$). **B,** Localization of
600 *Hv*ERdj3B in barley leaf epidermal cells. A ubiquitin promoter-driven expression construct
601 encoding *Hv*ERdj3B (w. SP) fused to the N-terminus of mYFP was co-transformed with an SP-
602 mCherry-HDEL construct into barley epidermal cells using particle bombardment. The cells were
603 observed by confocal laser scanning microscopy 48 h later. **C-F,** Localization of *Hv*ERdj3B in *N.*
604 *benthamiana* leaf epidermal cells using the split GFP system. *Hv*ERdj3B(w. SP)-GFP11 and SP-GFP1-
605 10-HDEL reconstitute reticulate fluorescent GFP, while GFP11-*Hv*ERdj3B (w/o SP) and GFP1-10
606 reconstitute cytosolic and nuclear fluorescent GFP. Expression constructs were introduced using
607 *Agrobacterium* infiltration, and epidermal cells were observed by laser scanning confocal
608 microscopy 48 h later. Size bars, 20 μm (B,C,F) and 40 μm (D,E).
609

610 **Figure 6. AVR_{A1} and BEC1016 localized in the cytosol and nucleus of *N. benthamiana* epidermal**
611 **cells.** Constructs for expression of effectors (w/o SP) were introduced using *Agrobacterium*
612 infiltration, and epidermal cells were observed by laser scanning confocal microscopy 48 h later.
613 Size bars, 40 μm.
614
615 **Figure 7. AVR_{A1} and BEC1016 are partially translocated into the ER lumen.** The GFP1-10/GFP11
616 self-constituting fluorescence protein demonstrates cytosolic and ER-luminal protein localizations
617 *N. benthamiana* epidermal cells. **A-B and I-J,** GFP11-CNX™ and CNX™-GFP11 confirm SP-GFP11-
618 HDEL to be ER-luminal and GFP1-10 to be cytosolic, respectively. **C-H and K-P,** AVR_{A1}, BEC1016 and
619 CSEP0105 (all w/o SP) are cytosolic while AVR_{A1} and BEC1016 (both w/o SP) are also ER-lumunal,
620 indicated by their reticulate and perinuclear signals (see also **Fig. S8**). Expression constructs were
621 introduced using *Agrobacterium* infiltration, and epidermal cells were observed by laser scanning
622 confocal microscopy 48 h later. Size bars, 40 μm.
623
624 **Supplemental Figure S1. Attempted alignment of the amino acid sequences of AVR_{A1}** (CSEP0008,
625 BLGH_03023) **and BEC1016** (CSEP0491, BLGH_07006)**.** Signal peptides underlined (black),
626 predicted beta sheets underlined (green), and intron position in the encoding genes indicated by
627 dashed line (orange).
628
629 **Supplemental Figure S2. Transcript accumulation on barley inoculated with *Bgh* isolate 5874. A,**
630 *Bgh* effector *AVRa1* (CSEP0008), **B,** *Bgh* effector *BEC1016* (CSEP0491) and **C,** barley target
631 *HvERdj3B* (HORVU1Hr1G022990) in wild-type progenitor CI 16151 (black solid lines) vs. fast-
632 neutron derived susceptible mutant *mla6*-m18982 (dashed red lines). *, significant difference
633 from CI 16151 at an adjusted $P < 0.001$ for barley genes. $P < 0.003$ for *Bgh*.
634
635 **Supplemental Figure S3. EtHAn-delivery of β-glucuronidase into barley leaf cells. A,** Leaf
636 infiltrated with EtHAn transformed with pEDV6-GUS. **B,** non-infiltrated leaf. The two leaves were
637 in parallel incubated in a GUS reaction buffer.
638

639 **Supplemental Figure S4. Y2H used to validate interactions between AVR_{A1}, BEC1016 and**
640 ***Hv*ERdj3B.** Binary confirmation of the interactions between AVR_{A1}, BEC1016 and *Hv*ERdj3B (aa
641 132-350), using the binary Y2H system described by Dreze *et al.* (2010) using DO-LW media as
642 diploid control and DO-LWH + 3AT as selection for positive interactions.
643
644 **Supplemental Figure S5. Bimolecular fluorescence complementation study of the interaction**
645 **between AVR_{A1}, BEC1016 and *Hv*ERdj3B.** These are the non-fluorescent combinations. The
646 fluorescent combinations are shown in **Fig. 4.** See legend of **Fig. 4** for more details. Size bars, 40
647 μm.
648
649 **Supplemental Figure S6. Subcellular localization of *Hv*ERdj3B in *N. benthamiana* epidermal cells.**
650 *Hv*ERdj3B (w. SP) gave reticular signal overlapping with the SP-mCherry-HDEL ER marker. Size bars,
651 10 μm.
652
653 **Supplemental Figure S7. Localization of AVR_{A1} and BEC1016 in barley leaf epidermal cells.**
654 Ubiquitin promoter-driven expression constructs encoding SP-free effectors (fused to the C-
655 terminus of mYFP) were co-transformed with a free mCherry construct into barley epidermal cells
656 using particle bombardment. The cells were observed by confocal laser scanning microscopy 48 h
657 later. Size bars, 10 μm.
658
659 **Supplemental Figure S8. BEC1016 can translocate into the ER.** Construct encoding BEC1016-
660 GFP11 (w/o SP) and SP-GFP1-10-HDEL were co-transformed into *N. benthamiana* leaves using
661 *Agrobacterium* infiltration, and epidermal cells were observed by laser scanning confocal
662 microscopy 48 h later. Size bars, 20 μm.
663
664 **Supplemental Table S1. Y2H-SCORES for the AVRA1 and BEC1016 baits.**
665
666 **Supplemental Table S2. Primer sequences for plasmid constructions (5´ to 3´).**
667
668

669

Parsed Citations

Aguilar GB, Pedersen C, Thordal-Christensen H (2016) Identification of eight effector candidate genes involved in early aggressiveness of the barley powdery mildew fungus. Plant Pathology 65: 953-958
Google Scholar: Author Only Title Only Author and Title

Ahmed AA, Pedersen C, Schultz-Larsen T, Kwaaitaal M, Jørgensen HJ, Thordal-Christensen H (2015) The barley powdery mildew candidate secreted effector protein CSEP0105 inhibits the chaperone activity of a small heat shock protein. Plant Physiology 168: 321-333
Google Scholar: Author Only Title Only Author and Title

Ahmed AA, Pedersen C, Thordal-Christensen H (2016) The barley powdery mildew effector candidates CSEP0081 and CSEP0254 promote fungal infection success. PLoS ONE 11, e0157586.
Google Scholar: Author Only Title Only Author and Title

Banerjee S, Velásquez-Zapata V, Fuerst G, Elmore JM, Wise RP (2021) NGPINT: a next-generation protein–protein interaction software. Briefings in Bioinformatics 22: bbaa351. DOI: 10.1093/bib/bbaa351
Google Scholar: Author Only Title Only Author and Title

Bauer S, Yu D, Lawson AW, Saur IM, Frantzeskakis L, Kracher B, Logemann E, Chai J, Maekawa T, Schulze-Lefert P (2021) The leucine-rich repeats in allelic barley MLA immune receptors define specificity towards sequence-unrelated powdery mildew avirulence effectors with a predicted common RNase-like fold. PLoS Pathogens 17: 1-36
Google Scholar: Author Only Title Only Author and Title

Benjamini Y, Hochberg Y 1995. Controlling the false discovery rate: A practical and powerful Approach to multiple testing. J R Stat Soc Ser B. 57: 289–300.
Google Scholar: Author Only Title Only Author and Title

Bindschedler LV, Burgis TA, Mills DJ, Ho JT, Cramer R, Spanu PD (2009) In planta proteomics and proteogenomics of the biotrophic barley fungal pathogen Blumeria graminis f. sp. hordei. Mol Cell Proteomics 8: 2368-2381.
Google Scholar: Author Only Title Only Author and Title

Carter ME, Helm M, Chapman AVE, Wan E, Restrepo Sierra AM, Innes RW, Bogdanove AJ, Wise RP (2019) Convergent evolution of effector protease recognition by Arabidopsis and barley. Molecular Plant-Microbe Interactions 32: 550-565.
Google Scholar: Author Only Title Only Author and Title

Chapman AVE, Hunt M, Surana P, Velásquez-Zapata V, Xu W, Fuerst G, Wise RP (2021) Disruption of barley immunity to powdery mildew by an in-frame Lys-Leu deletion in the essential protein SGT1. Genetics 217: iyaa026.
Google Scholar: Author Only Title Only Author and Title

Chen KC, Qu S, Chowdhury S, Noxon IC, Schonhoft JD, Plate L, Powers ET, Kelly JW, Lander GC, Wiseman RL (2017) The endoplasmic reticulum HSP 40 co-chaperone ERdj3/DNAJB11 assembles and functions as a tetramer. EMBO Journal 36: 2296-2309
Google Scholar: Author Only Title Only Author and Title

Douchkov D, Nowara D, Zierold U, Schweizer P (2005) A high-throughput gene-silencing system for the functional assessment of defense-related genes in barley epidermal cells. Molecular Plant-Microbe Interactions 18: 755-761
Google Scholar: Author Only Title Only Author and Title

Dreze M, Monachello D, Lurin C, Cusick ME, Hill DE, Vidal M, Braun P (2010) High-quality binary interactome mapping. Methods in Enzymology 470: 281-315
Google Scholar: Author Only Title Only Author and Title

Erffelinck ML, Ribeiro B, Perassolo M, Pauwels L, Pollier J, Storme V, Goossens A (2018) A user-friendly platform for yeast two-hybrid library screening using next generation sequencing. PLoS One 13: 1-21
Google Scholar: Author Only Title Only Author and Title

Fabro G, Steinbrenner J, Coates M, Ishaque N, Baxter L, Studholme DJ, Körner E, Allen RL, Piquerez SJ, Rougon-Cardoso A, Greenshields D, et al. (2011) Multiple candidate effectors from the oomycete pathogen Hyaloperonospora arabidopsidis suppress host plant immunity. PLoS Pathogen 7: 1-18
Google Scholar: Author Only Title Only Author and Title

Fan G, Yang Y, Li T, Lu W, Du Y, Qiang X, Wen Q, Shan W (2018) A Phytophthora capsici RXLR effector targets and inhibits a plant PPIase to suppress endoplasmic reticulum-mediated immunity. Molecular Plant 11: 1067-1083
Google Scholar: Author Only Title Only Author and Title

Fatima K, Naqvi F, Younas H (2021) A Review: Molecular Chaperone-mediated Folding, Unfolding and Disaggregation of Expressed Recombinant Proteins. Cell Biochemistry and Biophysics 79: 153-174
Google Scholar: Author Only Title Only Author and Title

Figueroa M, Ortiz D, Henningsen EC (2021) Tactics of host manipulation by intracellular effectors from plant pathogenic fungi. Currernt Opinion in Plant Biololgy 62: 102054
Google Scholar: Author Only Title Only Author and Title

Frantzeskakis L, Kracher B, Kusch S, Yoshikawa-Maekawa M, Bauer S, Pedersen C, Spanu PD, Maekawa T, Schulze-Lefert P, Panstruga R (2018) Signatures of host specialization and a recent transposable element burst in the dynamic one-speed genome of the fungal barley powdery mildew pathogen. BMC Genomics 19: 1-23
Google Scholar: Author Only Title Only Author and Title

Hu CD, Kerppola TK (2003) Simultaneous visualization of multiple protein interactions in living cells using multicolor fluorescence complementation analysis. Nature Biotechnology 21: 539-545
Google Scholar: Author Only Title Only Author and Title

Hunt M, Banerjee S, Surana P, Liu M, Fuerst G, Mathioni S, Meyers BC, Nettleton D, Wise RP (2019) Small RNA discovery in the interaction between barley and the powdery mildew pathogen. BMC Genomics 20: 610.
Google Scholar: Author Only Title Only Author and Title

Jin L, Mackey DM (2017) Measuring callose deposition, an indicator of cell wall reinforcement, during bacterial infection in Arabidopsis. Methods in Molecular Biology 1578: 195-205
Google Scholar: Author Only Title Only Author and Title

Jing M, Guo B, Li H, Yang B, Wang H, Kong G, Zhao Y, Xu H, Wang Y, Ye W, Dong S, et al. (2016) A Phytophthora sojae effector suppresses endoplasmic reticulum stress-mediated immunity by stabilizing plant binding immunoglobulin proteins. Nature Communications 7: 1-17
Google Scholar: Author Only Title Only Author and Title

Jones JD, Vance RE, Dangl JL (2016) Intracellular innate immune surveillance devices in plants and animals. Science 354: aaf6395
Google Scholar: Author Only Title Only Author and Title

Kamigaki A, Nito K, Hikino K, Goto-Yamada S, Nishimura M, Nakagawa T, Mano S (2016) Gateway vectors for simultaneous detection of multiple protein−protein interactions in plant cells using bimolecular fluorescence complementation. PLoS One 11: e0160717.
Google Scholar: Author Only Title Only Author and Title

Kanja C, Hammond-Kosack KE (2020) Proteinaceous effector discovery and characterization in filamentous plant pathogens. Molecular Plant Pathology 21: 1353-1376
Google Scholar: Author Only Title Only Author and Title

Keselman HJ, Algina J, Kowalchuk RK (2001) The analysis of repeated measures designs: A review. Br J Math Stat Psychol. 54: 1–20.
Google Scholar: Author Only Title Only Author and Title

Kourelis J, Van Der Hoorn RA (2018) Defended to the nines: 25 years of resistance gene cloning identifies nine mechanisms for R protein function. Plant Cell 30: 285-299
Google Scholar: Author Only Title Only Author and Title

Kørner CJ, Du X, Vollmer ME, Pajerowska-Mukhtar KM (2015) Endoplasmic reticulum stress signaling in plant immunity-at the crossroad of life and death. International Journal of Molecular Sciences 16: 26582-26598
Google Scholar: Author Only Title Only Author and Title

Lewis JD, Wan J, Ford R, Gong Y, Fung P, Nahal H, Wang PW, Desveaux D, Guttman DS (2012) Quantitative Interactor Screening with next-generation Sequencing (QIS-Seq) identifies Arabidopsis thaliana MLO2 as a target of the Pseudomonas syringae type III effector HopZ2. BMC Genomics 13: 1-13
Google Scholar: Author Only Title Only Author and Title

Li J, Zhao-Hui C, Batoux M, Nekrasov V, Roux M, Chinchilla D, Zipfel C, Jones JD (2009) Specific ER quality control components required for biogenesis of the plant innate immune receptor EFR. Proceedings of the National Academy of Sciences USA 106: 15973-15978
Google Scholar: Author Only Title Only Author and Title

Li X, Jin C, Yuan H, Huang W, Liu F, Fan R, Xie J, Shen QH (2021) The barley powdery mildew effectors CSEP0139 and CSEP0182 suppress cell death and promote B. graminis fungal virulence in plants. Phytopathology Research 3: 1-14
Google Scholar: Author Only Title Only Author and Title

Lu X, Kracher B, Saur IM, Bauer S, Ellwood SR, Wise R, Yaeno T, Maekawa T, Schulze-Lefert P (2016) Allelic barley MLA immune receptors recognize sequence-unrelated avirulence effectors of the powdery mildew pathogen. Proceedings of the National Academy of Sciences USA 113: E6486-E6495
Google Scholar: Author Only Title Only Author and Title

Lück S, Kreszies T, Strickert M, Schweizer P, Kuhlmann M, Douchkov D (2019) siRNA-Finder (si-Fi) software for RNAi-target

design and off-target prediction. Frontiers in Plant Science 10: 1023
Google Scholar: Author Only Title Only Author and Title

Menardo F, Praz CR, Wicker T, Keller B (2017) Rapid turnover of effectors in grass powdery mildew (Blumeria graminis). BMC Evolutionary Biology 17: 1-14
Google Scholar: Author Only Title Only Author and Title

Moreno AA, Mukhtar MS, Blanco F, Boatwright JL, Moreno I, Jordan MR, Chen Y, Brandizzi F, Dong X, Orellana A, Pajerowska-Mukhtar KM (2012) IRE1/bZIP60-mediated unfolded protein response plays distinct roles in plant immunity and abiotic stress responses. PLoS One 7: 1-15
Google Scholar: Author Only Title Only Author and Title

Mukhtar MS, Carvunis AR, Dreze M, Epple P, Steinbrenner J, Moore J, Tasan M, Galli M, Hao T, Nishimura MT, Pevzner SJ (2011) Independently evolved virulence effectors converge onto hubs in a plant immune system network. Science 333: 596-601
Google Scholar: Author Only Title Only Author and Title

Nekrasov V, Li J, Batoux M, Roux M, Chu ZH, Lacombe S, Rougon A, Bittel P, Kiss-Papp M, Chinchilla D, Van Esse HP, et al. (2009) Control of the pattern-recognition receptor EFR by an ER protein complex in plant immunity. EMBO Journal 28: 3428-3438
Google Scholar: Author Only Title Only Author and Title

Nelson BK, Cai X, Nebenführ A (2007) A multicolored set of in vivo organelle markers for co-localization studies in Arabidopsis and other plants. Plant Journal 51: 1126-1136
Google Scholar: Author Only Title Only Author and Title

Ngou BPM, Ding P, Jones JD (2022) Thirty years of resistance: Zig-zag through the plant immune system. Plant Cell doi: 10.1093/plcell/koac041
Google Scholar: Author Only Title Only Author and Title

Nowara D, Gay A, Lacomme C, Shaw J, Ridout C, Douchkov D, Hensel G, Kumlehn J, Schweizer P (2010) HIGS: host-induced gene silencing in the obligate biotrophic fungal pathogen Blumeria graminis. Plant Cell 22: 3130-3141
Google Scholar: Author Only Title Only Author and Title

Pashkova N, Peterson TA, Krishnamani V, Breheny P, Stamnes M, Piper RC (2016) DEEPN as an approach for batch processing of yeast 2-hybrid interactions. Cell Reports 17: 303-315
Google Scholar: Author Only Title Only Author and Title

Pedersen C, van Themaat EV, McGuffin LJ, Abbott JC, Burgis TA, Barton G, Bindschedler LV, Lu X, Maekawa T, Weßling R, Cramer R, et al. (2012) Structure and evolution of barley powdery mildew effector candidates. BMC Genomics 13: 1-21
Google Scholar: Author Only Title Only Author and Title

Pennington HG, Jones R, Kwon S, Bonciani G, Thieron H, Chandler T, Luong P, Morgan SN, Przydacz M, Bozkurt T, Bowden S, et al. (2019) The fungal ribonuclease-like effector protein CSEP0064/BEC1054 represses plant immunity and interferes with degradation of host ribosomal RNA. PLoS Pathogens 15: 1-33
Google Scholar: Author Only Title Only Author and Title

Pliego C, Nowara D, Bonciani G, Gheorghe DM, Xu R, Surana P, Whigham E, Nettleton D, Bogdanove AJ, Wise RP, Schweizer P, et al. (2013) Host-induced gene silencing in barley powdery mildew reveals a class of ribonuclease-like effectors. Molecular Plant-Microbe Interactions 26: 633-642
Google Scholar: Author Only Title Only Author and Title

Pobre KF, Poet GJ, Hendershot LM (2019) The endoplasmic reticulum (ER) chaperone BiP is a master regulator of ER functions: Getting by with a little help from ERdj friends. Journal of Biological Chemistry 294: 2098-2108
Google Scholar: Author Only Title Only Author and Title

Qiang X, Zechmann B, Reitz MU, Kogel KH, Schäfer P (2012) The mutualistic fungus Piriformospora indica colonizes Arabidopsis roots by inducing an endoplasmic reticulum stress–triggered caspase-dependent cell death. Plant Cell 24: 794-809
Google Scholar: Author Only Title Only Author and Title

Rasco-Gaunt S, Riley A, Barcelo P, Lazzeri PA (1999) Analysis of particle bombardment parameters to optimise DNA delivery into wheat tissues. Plant Cell Reports 19: 118-127
Google Scholar: Author Only Title Only Author and Title

Robertson M (2004) Two transcription factors are negative regulators of gibberellin response in the HvSPY-signaling pathway in barley aleurone. Plant Physiology 136: 2747-2761
Google Scholar: Author Only Title Only Author and Title

Saur IM, Bauer S, Kracher B, Lu X, Franzeskakis L, Müller MC, Sabelleck B, Kümmel F, Panstruga R, Maekawa T, Schulze-Lefert P (2019) Multiple pairs of allelic MLA immune receptor-powdery mildew AVRA effectors argue for a direct recognition mechanism. Elife 8: 1-31
Google Scholar: Author Only Title Only Author and Title

Schindelin J, Arganda-Carreras I, Frise E, Kaynig V, Longair M, Pietzsch T, Preibisch S, Rueden C, Saalfeld S, Schmid B, Tinevez JY, et al. (2012) Fiji: an open-source platform for biological-image analysis. Nat Methods. 9: 676-82
Google Scholar: Author Only Title Only Author and Title

Seeholzer S, Tsuchimatsu T, Jordan T, Bieri S, Pajonk S, Yang W, Jahoor A, Shimizu KK, Keller B, Schulze-Lefert P (2010) Diversity at the Mla powdery mildew resistance locus from cultivated barley reveals sites of positive selection. Molecular Plant-Microbe Interactions 23: 497-509
Google Scholar: Author Only Title Only Author and Title

Sivamani E, DeLong RK, Qu R (2009) Protamine-mediated DNA coating remarkably improves bombardment transformation efficiency in plant cells. Plant Cell Reports 28: 213-221
Google Scholar: Author Only Title Only Author and Title

Sohn KH, Lei R, Nemri A, Jones JD (2007) The downy mildew effector proteins ATR1 and ATR13 promote disease susceptibility in Arabidopsis thaliana. Plant Cell 19: 4077-4090
Google Scholar: Author Only Title Only Author and Title

Spanu PD, Abbott JC, Amselem J, Burgis TA, Soanes DM, et al. (2010). Genome expansion and gene loss in powdery mildew fungi reveal tradeoffs in extreme parasitism. Science 330: 1543-1546.
Google Scholar: Author Only Title Only Author and Title

Spanu PD (2017). Cereal immunity against powdery mildews targets RNase-Like Proteins associated with Haustoria (RALPH) effectors evolved from a common ancestral gene. New Phytologist 213: 969-971
Google Scholar: Author Only Title Only Author and Title

Sun Y, Zhu YX, Balint-Kurti PJ, Wang GF (2020) Fine-tuning immunity: players and regulators for plant NLRs. Trends in Plant Science 25: 695-713
Google Scholar: Author Only Title Only Author and Title

Surana P (2017) Membrane trafficking in resistance gene-mediated defense against the barley powdery mildew fungus (Doctoral dissertation, Iowa State University)

Suter B, Zhang X, Pesce CG, Mendelsohn AR, Dinesh-Kumar SP, Mao JH (2015) Next-generation sequencing for binary protein–protein interactions. Frontiers in Genetics 6: 1-6
Google Scholar: Author Only Title Only Author and Title

Thomas WJ, Thireault CA, Kimbrel JA, Chang JH (2009) Recombineering and stable integration of the Pseudomonas syringae pv. syringae 61 hrp/hrc cluster into the genome of the soil bacterium Pseudomonas fluorescens Pf0-1. Plant Journal 60: 919-928
Google Scholar: Author Only Title Only Author and Title

Thordal-Christensen H (2020) A holistic view on plant effector-triggered immunity presented as an iceberg model. Cellular and Molecular Life Sciences 10: 1-14
Google Scholar: Author Only Title Only Author and Title

Tintor N, Saijo Y (2014) ER-mediated control for abundance, quality, and signaling of transmembrane immune receptors in plants. Frontiers in Plant Science 5: 65
Google Scholar: Author Only Title Only Author and Title

Trigg SA, Garza RM, MacWilliams A, Nery JR, Bartlett A, Castanon R, Goubil A, Feeney J, O'Malley R, Shao-shan CH, Zhang ZZ, et al. (2017) CrY2H-seq: a massively multiplexed assay for deep-coverage interactome mapping. Nature Methods 14: 819-825
Google Scholar: Author Only Title Only Author and Title

Upadhyaya NM, Ellis JG, Dodds PN (2014) A bacterial type III secretion-based delivery system for functional assays of fungal effectors in cereals. Methods in Molecular Biology 1127: 277-290
Google Scholar: Author Only Title Only Author and Title

van Wersch S, Tian L, Hoy R, Li X (2020) Plant NLRs: the whistleblowers of plant immunity. Plant Communications 1: 100016
Google Scholar: Author Only Title Only Author and Title

Velásquez-Zapata V, Elmore JM, Banerjee S, Dorman KS, Wise RP (2021) Next-generation yeast-two-hybrid analysis with Y2H-SCORES identifies novel interactors of the MLA immune receptor. PLoS Computational Biology 17: e1008890. DOI: 10.1371/journal.pcbi.1008890
Google Scholar: Author Only Title Only Author and Title

Velásquez-Zapata V, Elmore JM, Fuerst GS, Wise RP (2022) An interolog-based barley interactome as an integration framework for NLR immune signaling. Genetics: iyac056, https://doi.org/10.1093/genetics/iyac056.
Google Scholar: Author Only Title Only Author and Title

Voigt CA (2014) Callose-mediated resistance to pathogenic intruders in plant defense-related papillae. Frontiers in Plant Science 5: 168

Google Scholar: Author Only Title Only Author and Title

Voigt CA (2016) Cellulose/callose glucan networks: the key to powdery mildew resistance in plants? New Phytologist 212: 303-305
Google Scholar: Author Only Title Only Author and Title

Voinnet O, Rivas S, Mestre P, Baulcombe D (2003) Retracted: An enhanced transient expression system in plants based on suppression of gene silencing by the p19 protein of tomato bushy stunt virus. Plant Journal 33: 949-956
Google Scholar: Author Only Title Only Author and Title

Wang J, Dhroso A, Liu X, Baum TJ, Hussey RS, Davis EL, Wang X, Korkin D, Mitchum MG (2021) Phytonematode peptide effectors exploit a host post-translational trafficking mechanism to the ER using a novel translocation signal. New Phytologist 229: 563-574
Google Scholar: Author Only Title Only Author and Title

Wang Z, Li X, Wang X, Liu N, Xu B, Peng Q, Guo Z, Fan B, Zhu C, Chen Z (2019) Arabidopsis endoplasmic reticulum-localized UBAC2 proteins interact with PAMP-INDUCED COILED-COIL to regulate pathogen-induced callose deposition and plant immunity. Plant Cell 31: 153-171
Google Scholar: Author Only Title Only Author and Title

Weimann M, Grossmann A, Woodsmith J, Özkan Z, Birth P, Meierhofer D, Benlasfer N, Valovka T, Timmermann B, Wanker EE, Sauer S (2013) A Y2H-seq approach defines the human protein methyltransferase interactome. Nature Methods 10: 339-342
Google Scholar: Author Only Title Only Author and Title

Weßling R, Epple P, Altmann S, He Y, Yang L, Henz SR, McDonald N, Wiley K, Bader KC, Gläßer C, Mukhtar MS, et al. (2014) Convergent targeting of a common host protein-network by pathogen effectors from three kingdoms of life. Cell Host & Microbe 16: 364-375
Google Scholar: Author Only Title Only Author and Title

Xie W, Nielsen ME, Pedersen C, Thordal-Christensen H (2017) A split-GFP gateway cloning system for topology analyses of membrane proteins in plants. PloS One 12: 1-8
Google Scholar: Author Only Title Only Author and Title

Xu Q, Tang C, Wang L, Zhao C, Kang Z, Wang X (2020) Haustoria-arsenals during the interaction between wheat and Puccinia striiformis f. sp. tritici. Molecular Plant Pathology 21: 83-94
Google Scholar: Author Only Title Only Author and Title

Xu W, Meng Y, Surana P, Fuerst G, Nettleton D, Wise RP (2015) The knottin-like Blufensin family regulates genes involved in nuclear import and the secretory pathway in barley-powdery mildew interactions. Frontiers in Plant Science 6: 409.
Google Scholar: Author Only Title Only Author and Title

Xu G, Zhong X, Shi Y, Liu Z, Jiang N, Liu J, Ding B, Li Z, Kang H, Ning Y, Liu W, et al. (2020) A fungal effector targets a heat shock–dynamin protein complex to modulate mitochondrial dynamics and reduce plant immunity. Science Advances 6: 1-10.
Google Scholar: Author Only Title Only Author and Title

Yachie N, Petsalaki E, Mellor JC, Weile J, Jacob Y, Verby M, Ozturk SB, Li S, Cote AG, Mosca R, Knapp JJ, et al. (2016) Pooled-matrix protein interaction screens using Barcode Fusion Genetics. Molecular Systems Biology 12: 863
Google Scholar: Author Only Title Only Author and Title

Yamamoto M, Maruyama D, Endo T, Nishikawa SI (2008) Arabidopsis thaliana has a set of J proteins in the endoplasmic reticulum that are conserved from yeast to animals and plants. Plant and Cell Physiology 49: 1547-1562
Google Scholar: Author Only Title Only Author and Title

Yu CP, Chen SC, Chang YM, Liu WY, Lin HH, Lin JJ, Chen HJ, Lu YJ, Wu YH, Lu MY, Lu CH, et al. (2015) Transcriptome dynamics of developing maize leaves and genomewide prediction of cis elements and their cognate transcription factors. Proceedings of the National Academy of Sciences USA 112: E2477-E2486
Google Scholar: Author Only Title Only Author and Title

Yuan M, Jiang Z, Bi G, Nomura K, Liu M, Wang Y, Cai B, Zhou JM, He SY, Xin XF (2021a) Pattern-recognition receptors are required for NLR-mediated plant immunity. Nature 592: 105-109
Google Scholar: Author Only Title Only Author and Title

Yuan H, Jin C, Pei H, Zhao L, Li X, Li J, Huang W, Fan R, Liu W, Shen QH (2021b) The powdery mildew effector CSEP0027 interacts with barley catalase to regulate host immunity. Front Plant Sci. 12: 733237
Google Scholar: Author Only Title Only Author and Title

Zhang WJ, Pedersen C, Kwaaitaal M, Gregersen PL, Mørch SM, Hanisch S, Kristensen A, Fuglsang AT, Collinge DB, Thordal-Christensen H (2012) Interaction of barley powdery mildew effector candidate CSEP0055 with the defence protein PR17c. Molecular Plant Pathology 13: 1110-1119.
Google Scholar: Author Only Title Only Author and Title

Zhang W-J, Hanisch S, Kwaaitaal M, Pedersen C, Thordal-Christensen H (2013) A component of the Sec61 ER protein transporting pore is required for plant susceptibility to powdery mildew. Frontiers in Plant Science 4: 127.

Google Scholar: Author Only Title Only Author and Title

Zhong X, Yang J, Shi Y, Wang X, Wang GL (2018) The DnaJ protein OsDjA6 negatively regulates rice innate immunity to the blast fungus Magnaporthe oryzae. Molecular Plant Pathology 19: 607-614
Google Scholar: Author Only Title Only Author and Title

Zimmermann R, Eyrisch S, Ahmad M, Helms V (2021) Protein translocation across the ER membrane. Biochimica et Biophysica Acta 1808: 912–924
Google Scholar: Author Only Title Only Author and Title

Zipfel C, Oldroyd GE (2017) Plant signalling in symbiosis and immunity. Nature 543: 328-336
Google Scholar: Author Only Title Only Author and Title